## CHAPTER II

### 2. Designing, Synthesis and Biological evaluation of imidazo-quinoline derivatives as PI3Kδ selective inhibitors.

As discussed in chapter I, inhibition of PI3K is considered as one of the most interesting target for the safe and effective treatment of RA and cancer. However, knowing the potential side effects associated with PI3K$\alpha$ and $\beta$ isoforms inhibition (due to universal expression); recently, more efforts are directed towards the development of isoform selective inhibitors, particularly PI3K$\delta$ selective inhibitors, for the safe and effective treatment of RA and B-cell CLL.

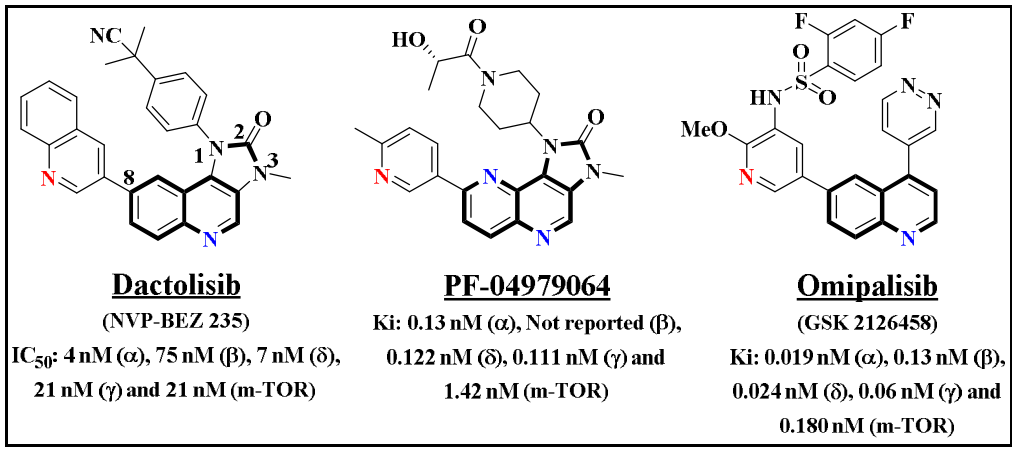


**Figure 14:** Quinoline and imidazo-quinoline based PI3K inhibitors

Over the past decades, several structurally diverse PI3K inhibitors are identified containing quinoline and imidazo quinoline as promising pharmacophore. The Omipalisib **[59]**, PF-04979064**[60]** and Dactolisib **[61]**, discovered by GlaxoSmithKline, Pfizer and Novartis respectively, as dual PI3K and mTOR inhibitors are under clinical trials**, Figure 14**. Omipalisib (GSK2126458) is a quinoline based PI3K inhibitors, which showed good PI3K inhibitory activity against all the four PI3K isoforms and mTOR ($IC_{50}$< 0.2 nM)

along with the potent anti-tumor activity *in vivo*. PF-04979064 and Dactolisib are dual PI3K/mTOR inhibitors, designed based on imidazo-quinoline scaffold. Dactolisib possess $IC_{50}$ values of 4, 75, 7, 5 and 21 nM against PI3Kα, PI3Kβ, PI3Kδ, PI3Kγ and mTOR, respectively **[62]**.

Initially we analysed the crystal structures of Dactolisib in PI3Kδ ATP binding pocket, PDB ID: **2WXK**, **Figure 15**. We found that the nitrogen (blue) of imidazo-quinoline core forms a hydrogen bond with the backbone of $Val_{882}$, in the hinge region, while the nitrogen (red) of quinoline ring interacts with $Asp_{841}$, in affinity region. These hydrogen bonding interactions are essential for compounds to exhibit PI3K inhibitory activities. Considering the above observation we selected imidazo-quinoline moiety as a starting point. Imidazo forms π- π stacking interaction with $Trp_{760}$, in specificity pocket. Thus, extension towards hydrophobic region is missing in the Dactolisib. Hence, appropriate structural modifications were carried out in the Dactolisib (pan-PI3K/mTOR inhibitor) to improve PI3K isoform selectivity, particularly to get PI3Kδ isoform selectivity.

In this chapter, we described design of PI3Kδ selective inhibitors starting from imidazo-quinoline as a pharmacophore. Core imidazo-quinoline structure was retained in the novel inhibitors and suitable modifications were carried out to retain all key interactions in the ATP binding pocket especially, in the hinge region, specificity pocket, affinity pocket and hydrophobic region of PI3Kδ enzyme.

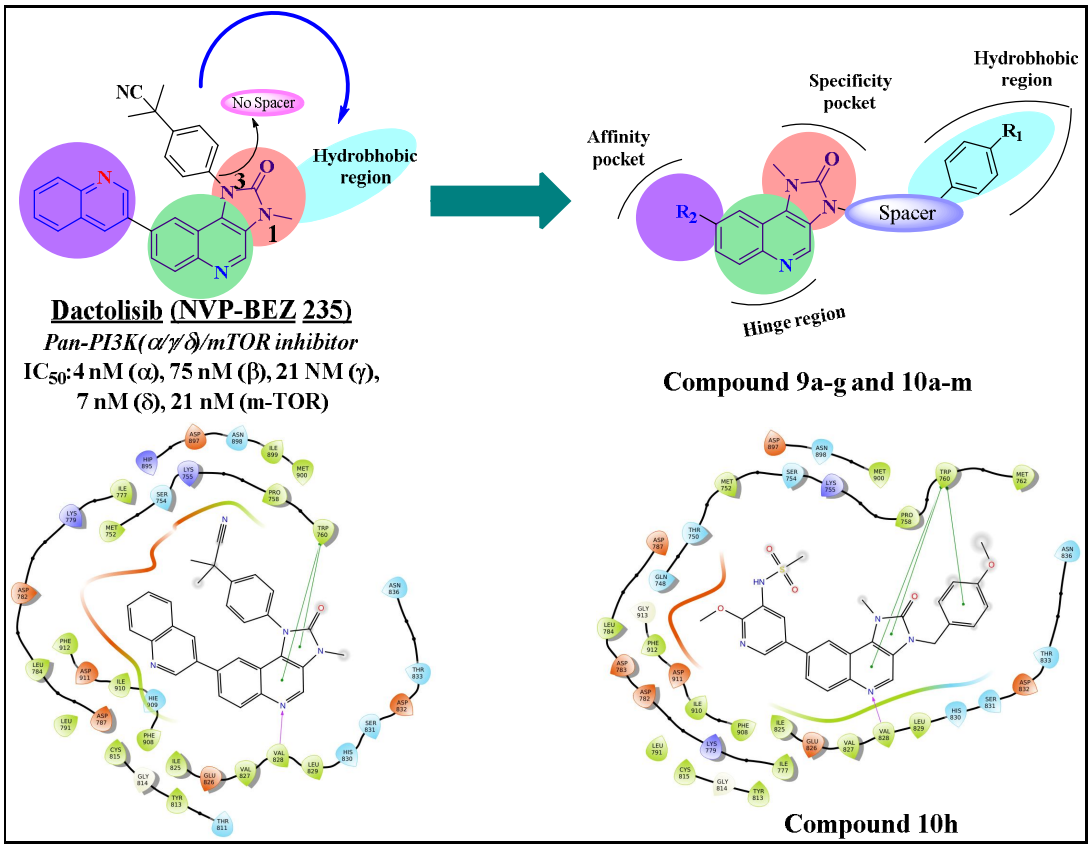


**Figure 15:** Designing strategy using imidazo-quinoline pharmacophore

Initial modifications were carried out on imidazole ring of Dactolisib, mainly by reversing the positions of methyl ($N^1$ to $N^3$) and phenyl ($N^3$ to $N^1$) groups and we also introduced carbon spacer (phenyl to benzyl) at $N^3$ position to make compound more flexible so that phenyl substitution can favour interaction in the hydrophobic region. Further appropriate modifications were carried out at the *p*-position of benzyl ring to obtain the single digit nM potency (**9c**). Compound **9c** was found to be potent but showed moderate isoform selectivity. So, in the second set, suitable modifications were carried out on the 8$^{th}$ position of **9c** to improve isoform selectivity and *in vivo* profile. All the test compounds synthesized were screened *in vitro* for PI3Kδ inhibitory activity and most potent compounds from each set were subjected for *in vitro* PI3K isoform

selectivity (α, β & γ) and mTOR inhibitory activity. Based on the *in vitro* results, highly potent and selective compound (**10h**) was subjected for *in vivo* Pharmacokinetic (PK) and Pharmacodynamics (PD) studies **[63]**.

## 2.1. Chemistry

### 2.1.1. Materials and Methods

All reagents used were obtained from Sigma Aldrich and were used without further purification. Solvents were purchased from a commercial source and used after distilling or drying according to the known methods. All the air and/or moisture sensitive reactions were carried out in dry solvents, under the nitrogen atmosphere. Melting points were recorded in open glass capillaries, using a scientific melting point apparatus (Mettler Toledo, Switzerland) and are uncorrected.

The $^{1}H$ NMR spectra were recorded on a Bruker Avance-400 (400MHz) spectrometer, Switzerland. The chemical shifts (δ) are reported in parts per million (ppm) relative to TMS (tetramethylsilane), either in $CDCl_3$, $CD_3OD$ or DMSO-$d_6$. Signal multiplicities are represented as s (singlet), d (doublet), dd (doublet of doublet), t (triplet), q (quartet), bs (broad singlet), and m (multiple). $^{13}C$ NMR spectra were recorded on Bruker Avance-400 at 100 MHz either in $CDCl_3$, MeOH or DMSO-$d_6$.

Mass spectra (ESI-MS) were obtained on Shimadzu LCMS 2010-A spectrometer, Japan. Elemental analyses were carried out, using a Perkin-Elmer 2400 CHN analyser, UK. UPLC analysis were carried out at λmax 220nm, using column YMC-Triart C18 (100*2.0 mm) on Water acquity UPLC, Europe (Austria).

Progress of the reactions was monitored by TLC, using Pre coated TLC plates (E. Merck Kiesegel 60 F254, Germany) and the spots were visualized by UV and/or iodine vapours. The chromatographic purification was performed on silica gel (230-400 mesh). Few compounds directly used for the next step without purification and analysis. In the next section, we have highlighted the importance of imidazo-quinoline pharmacophore and possible routes for the synthesis of imidazo-quinoline.

### 2.1.2. Importance of imidazo-quinoline in biological system

#### 2.1.2.1. Imidazo-quinoline as therapeutic agent

Imidazo-quinoline is a tricyclic ring containing 1,3-dihydro **imidazole** and **quinoline** ring fused together. Imidazo-quinoline possesses many therapeutic applications such as anticancer, antimalarial, antibacterial, antiproliferative, antiallergic, antiparasitic and anxiolytic properties. Some of them are listed below:

- **Example 1**

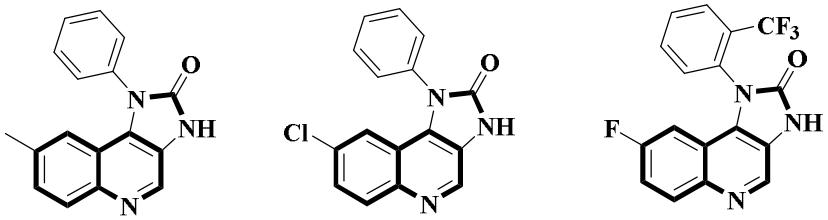


**Example 1a** **Example 1b** **Example 1c**

**Figure 16:** Imidazo-quinoline based antibacterial agents

Ladani et al. reported many substituted imidazo-quinoline based antibacterial compounds, which were evaluated *in vitro* against bacterial strains of *Streptococcus pneumoniae*, *Bacillus subtilis*, *Clostridium tetani* (gram positive), *Escherichia coli*, *Salmonella Typhi*, *Vibrio cholerae* (gram negative)

and antitubercular activity using *Mycobacterium tuberculosis* H37Rv strain. **Example 1a** and **1b** were found to be most potent against *S. pneumonia*, *B. subtilis* and *C. tetani*, whereas example **1c** showed 99% inhibition against *M. Tuberculosis*, MIC (minimum inhibitory concentration) of 42 μM**, Figure 16 [64]**.

- **Example 2**

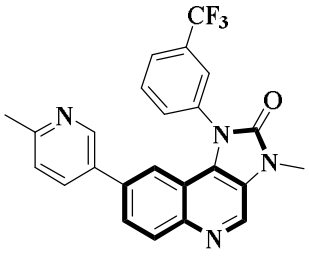


**Example 2**

**Figure 17:** Imidazo-quinoline based antimalarial agents

Patel et al. reported imidazo-quinoline as potent antimalarial agents against *Plasmodium falciparum*. **Example 2** showed excellent antimalarial activity with $IC_{50}$ of 21nM and 81nM for asexual parasite and gametocytes respectively, **Figure 17 [65]**.

- **Example 3**

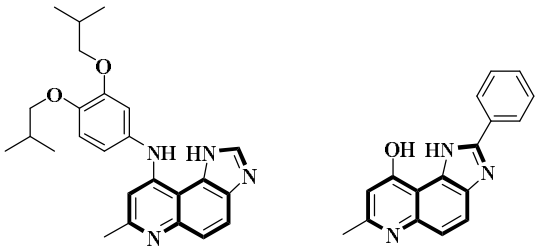


**Example 3a** **Example 3b**

**Figure 18:** Imidazo-quinoline based anthelmintic agent

Spencer et al. tested imidazo-quinoline derivatives against the tapeworm (*Hymenolepis nana*), **Figure 18**. **Example 3a** and **3b showed** 94 % and 84 % inhibitions, whereas reference compound Bunamidine showed 50 % inhibition respectively **[66]**.

- **Example 4**

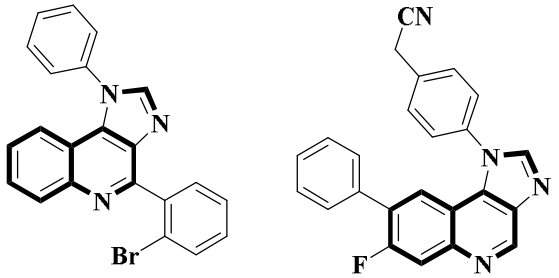


**Example 4a** **Example 4b**

**Figure 19:** Imidazo-quinoline based anticancer agent

Thigulla et al. reported 1,4-disubstituted imidazo-quinoline as anticancer agents in murine melanoma B16F10 cells, **Figure 19**. **Example 4a** was found to be most potent compound with $IC_{50}$ 103 μM **[67]**. N. Senthilkumar et al. reported **Example 4b** 2-(4-(7-f1uoro-8-phenyl-IH-imidazo[4,5-c]quinolin-l-yl)phenyl)acetonitrile as anticancer agent against the human breast cancer cell line MCF-7 (Michigan Cancer Foundation-7) 33% inhibition **[68]**.

- **Example 5** and **Example 6**

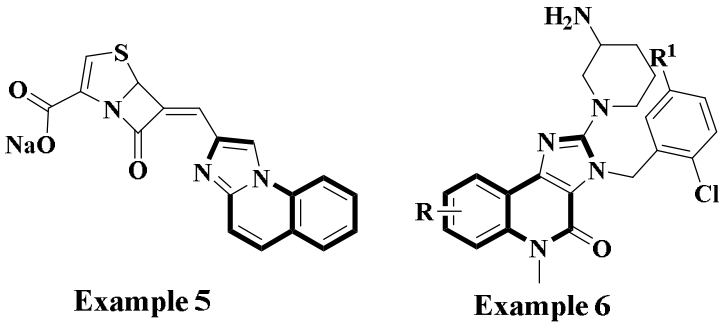


**Example 5** **Example 6**

**Figure 20:** Imidazo-quinoline based β-lactamase inhibitors

Venkatesan et al. reported tricyclic 6-methylidene penems as β-lactamase inhibitors, **Figure 20**. Fused penem with imidazo-quinoline scaffold, **example 5** showed potent inhibition of TEM-1 and Amp-C enzymes (β-lactamase enzyme) with $IC_{50}$ values of 3.4 and 2.1nM, respectively **[69]**.

Yohei et al. reported imidazo-quinoline derivative as novel, potent and selective DPP4 (dipeptidyl peptidase IV) inhibitors for the treatment of type 2 diabetes (T2D). **Example 6**, **Figure 20,** (R= 7-COOH, $R^1$=F) showed excellent DPP4 inhibitory activity and it was found to be selective against other DPP enzymes **[70]**.

### 2.1.2.2. Possible routes for the synthesis of imidazo-quinoline derivatives

Imidazo-quinoline contains imidazole ring fused to quinoline ring at different faces, forming different isomers, **Figure 21(a)**. From our research point, we were focused on *1/3H*-imidazo[4,5-c]quinoline (consider as imidazo-quinoline throughout thesis) ring system.

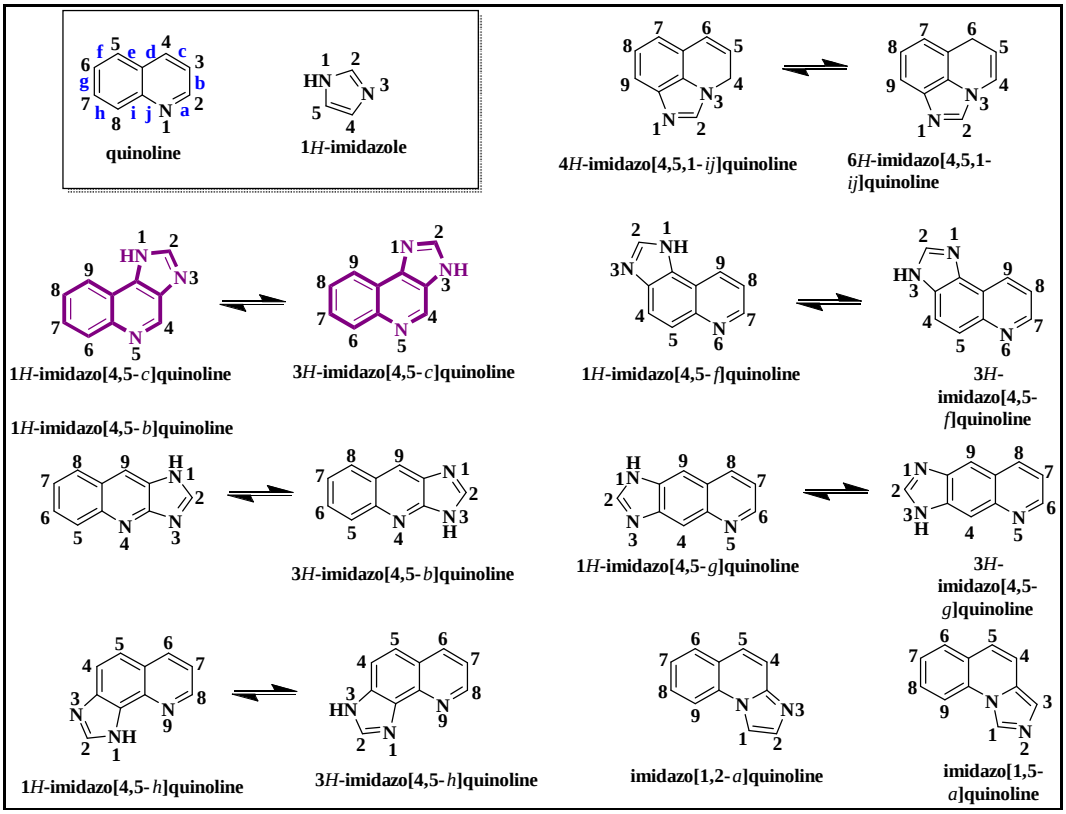


**Figure 21 (a):** Imidazo-quinoline: different isomers

In general, Imidazo-quinoline derivatives can be prepared by two main routes, **Figure 21 (b).** In the first route substituted diamine quinoline can be cyclise using diphosgene to get 1,3-dihydro imidazo-quinoline **[71]**. In the second route, 1,3-dihydro imidazo-quinoline can be synthesised from 4-amino-3-amido quinoline via Hofmann rearrangement and intramolecular cyclization, using iodobenzene diacetate **[72]**.

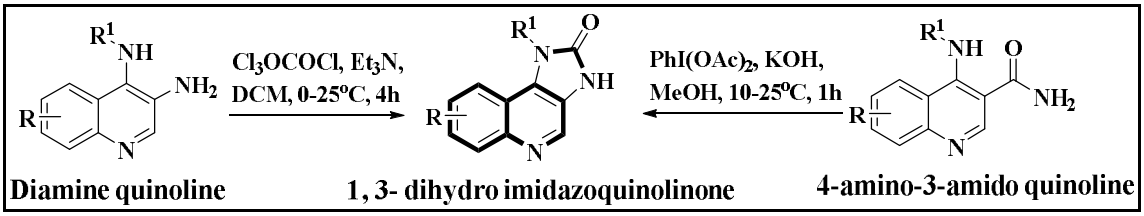


**Figure 21 (b):** Common routes for the preparation of imidazo-quinoline

As described in the earlier section, imidazo[4,5-c]quinoline is a privilege pharmacophore with versatile application in drug designing and discovery. We selected imidazo-quinoline as centre pharmacophore because it is known to exhibit PI3K inhibitory activity (Dactolisib). As described in the designing section (Chapter I), we tried to incorporate PI3Kδ selectivity by introducing suitable substitution. Over all we prepared 20 compounds (**9a-g** and **10a-l**), in two set. In the next section, we described synthetic scheme and experimental procedure for intermediates, and final compounds.

### 2.1.3. General procedure of the synthesis of title compounds 9a-g and 10a-l

Synthesis of 1,3-dihydro-2*H*-imidazo[4,5-c]quinoline-2-one derivatives (**9a-g** and**10a-l**) was carried out as depicted in Scheme 1, following the modified literature procedure**[71-72]**.Treatment of bromo anthranilic acid (**1**) with nitro methane gives nitro vinyl anthranilic acid (**2**).Probable reaction mechanism for this conversion is through key intermediate 2-nitroacetaldehyde. In first step, two moles of nitromethane reacts with NaOH to give dinitroethene, which is hydrolysed to 2-nitroacetaldehyde oxime (methazonic acid) in acidic medium which upon dehydration generates reactive 2-nitroacetaldehyde. (E)-5-bromo-2-((2-nitrovinyl) amino) benzoic acid **(2)** was cyclized using potassium acetate in acetic anhydride to get the 6-bromo-3-nitroquinolin-4-ol **3** by modified Niementowski quinoline synthesis. Compound **3** was converted to reactive chloro derivate **4** using $POCl_3$, followed by treatment with methyl amines to get the compound **5**, by nucleophilic substitution of the chloride with methyl amine. Subsequently, nitro group of compound **5** was reduced, using $SnCl_2$ to get the compound **6,** which was cyclized using diphosgene, in the presence of base, to obtain the imidazo-quinoline **7**. Alkylation of **7** using different substituted aryl halides with strong base furnished compounds **8a-g**,

which were further converted into the title compounds **9a-g** and **10a-l** by Suzuki reaction, using $PdCl_2(PPh_3)_2$, potassium bicarbonate and different aryl or heteroaryl boronic acids.

Some aryl or heteroaryl boronic acids/esters were procured from commercial sources (Aldrich, TCI); some of them were used from in house compound library and rest of the boronate acids/esters were prepared in house using modified literature procedure. Synthesis of N-(2-methoxy-5-(4,4,5,5-tetramethyl-1,3,2-dioxaborolan-2-yl)pyridin-3 yl)methanesulfonamide (16) is reported in detail 2.1.4 section in this chapter.

**Scheme 1**: Synthesis of compounds **9a-g** and **10a-l**

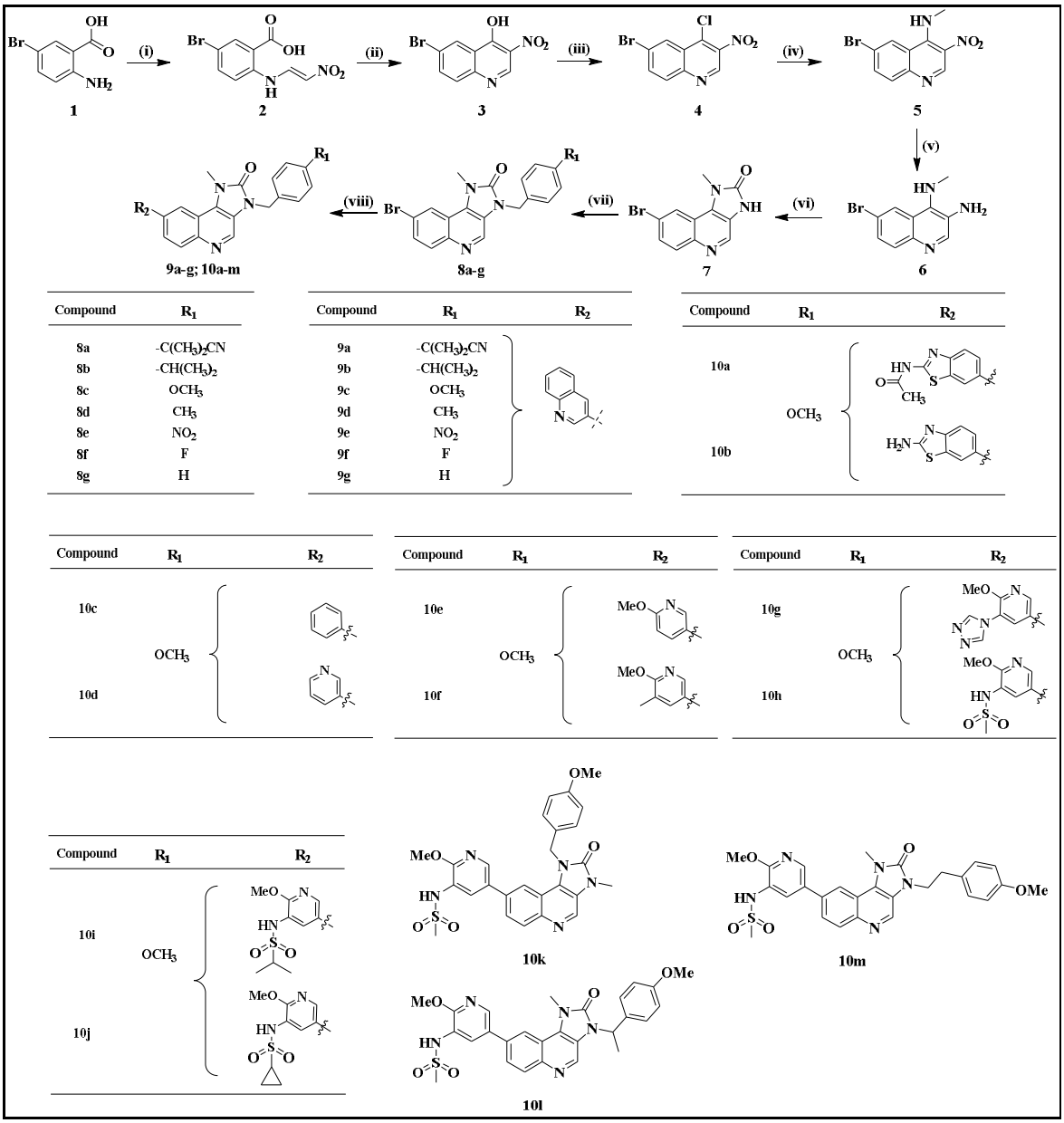


**Reagents and conditions:** i) conc. HCl, water, 26 $^{o}$C,6 h, then nitro methane, NaOH, water, conc. HCl, 26 $^{o}$C,16 h; ii) KOAc, acetic anhydride, 120-125 $^{o}$C,4 h; iii) $POCl_3$, 120 $^{o}$C, 4 h; iv) Me-$NH_2$, TEA, DCM, 26 $^{o}$C, 12 h; v) $SnCl_2.2(H_2O)$, EtOAc, 26 $^{o}$C, 4 h; vi) Phosgene (20% in toluene), TEA, DCM, 0-26 $^{o}$C, 30 min; vii) $R_1$-Ar-$CH_2$-X (Cl or Br), NaH, THF, 0-26 $^{o}$C, 1 h; viii) $R_2$-$B(OH)_2$,$PdCl_2(PPh_3)_2$, $KHCO_3$, DMF, $H_2O$, 90-95 $^{o}$C, 1.5 h.

**2.1.3.1. Detailed stepwise experimental procedure for synthesis title compounds 9a-g and 10a-l.**

**Step I:** Preparation of 5-Bromo-2-(2-nitro-vinylamino)-benzoic acid **2.**

A suspension of 2-amino-5-bromobenzoic acid **1** (5 g, 23.14 mmol) in $H_2O$: HCl (37%) was stirred for 8 h and then filtered **(Solution A).** Nitromethane (22.60 g, 370 mmol) was added to an ice-bath cooled mixture of ice (35 gm) and NaOH (15.3 g, 382 mmol). After stirring for 2 h at 0 $^oC$ to room temperature, to this solution ice (6 gm) and HCl (37%) (8 ml) were added at 0 $^oC$ to **(Solution B).**

Solution **A** and **B** were combined. Reaction mixture was stirred for 18 h. at room temperature. The yellow precipitate was filtered, washed with water (2 X 100 ml) followed by drying under vacuum to give 5-Bromo-2-(2-nitro-vinylamino)-benzoic acid **2** as yellow solid (5.1 g, Yield: 77 %).

**$^1$H NMR** (DMSO-$d_6$, 400 MHz) δ ppm: 6.78 (d, $J$ = 4 Hz, 1H), 7.73 (d, $J$ = 9.2 Hz, 1H), 7.85 (dd, $J_1$ = 9.2 Hz, $J_2$ = 2.8 Hz, 1H), 8.01-8.06 (m, 1H), 8.07 (d, $J$ = 2.4 Hz, 1H), 12.97 (d, $J$ = 13.6 Hz, 1H). **ESI-MS:** 284.8 $[M]^-$, 286.7 $[M+2]^-$. **Purity** (UPLC): 96.67%.

**Step II:** Preparation of 6-bromo-3-nitroquinolin-4-ol **3**.

5-bromo-((2-nitrovinyl) amino) benzoic acid **2** (2.9 g, 10.1 mmol) and potassium acetate (1.19 g, 12.1 mmol) in acetic anhydride (12.9 ml, 15.2 mmol) was stirred for 1.5 h at 120 $^oC$ The precipitate formed during reaction was filtered and washed with acetic acid until the filtrate was colourless. This white solid was washed with water and dried in vacuum to give 6-bromo-3-nitroquinolin-4-ol **3** as off white solid(1.22 g, Yield: 45 %).

**$^1$H NMR** (DMSO-$d_6$, 400 MHz) δ ppm: 7.68 (d, $J$ = 8.8 Hz, 1H), 7.95 (dd, $J_1$ = 8.8 Hz, $J_2$ = 2.2 Hz, 1H), 8.31 (d, $J$ = 4 Hz, 1H), 9.25 (s, 1H), 13.15 (br s, 1H). **ESI-MS:** 268.8 $[M]^+$, 270.8 $[M+2]^+$. **Purity** (UPLC): 99.19%.

**Step III:** Preparation of 6-bromo-4-chloro-3-nitroquinoline **4**.

6-bromo-3-nitroquinolin-4-ol **3** (2.0 g, 6.95 mmol) in $POCl_3$ (15 ml) was refluxed for 45 min at 120 $^oC$. The reaction mixture was cooled to room temperature and poured slowly into ice water. The precipitate was filtered, washed with ice-cold water and dissolved in DCM. The organic phase was washed with cold brine, and the aqueous phase was discarded. DCM layer was dried over sodium sulphate, and evaporated to dryness to provide the desired compound **4** as white solid (1.92 g, Yield: 90 %).

**$^1$H NMR** (DMSO-$d_6$, 400 MHz) δ ppm: 8.01 (dd, $J_1$ = 2.4 Hz, $J_2$ = 9.2 Hz, 1H), 8.10 (d, $J$ = 9.2 Hz, 1H), 8.59 (d, $J$ = 2 Hz, 1H), 9.25 (s, 1H). **ESI-MS:** 288.7 $[M+H]^+$. **Purity** (UPLC): 94.53 %.

**Step IV:** 6-bromo-N-methyl-3-nitroquinolin-4-amine **5**.

6-bromo-4-chloro-3-nitroquinoline **4** (5.0 g, 17.39 mmol) was dissolved in THF (10 ml), triethylamine (2.11 g, 20.87 mmol) was added followed by adding methyl amine (5 ml) aqueous solution. Reaction mixture was stirred for 12 h. at room temperature. Reaction mixture was concentrated to give yellow precipitate. Cold water (40 ml) was added, filtered and washed with water. The yellow solid obtained was dried in vacuum which to give the title compound **5** as yellow solid (4.2 g, Yield: 86%).

**$^1$H NMR** (DMSO-$d_6$, 400 MHz) δ ppm: 3.00 (s, 3H), 7.82 (d, $J$ = 8.8 Hz, 1H), 7.95 (dd, $J_1$ = 8.8 Hz, $J_2$ = 2 Hz, 1H), 8.71 (d, $J$ = 4 Hz, 1H), 8.88 (br s, 1H),

8.95 (d, *J* = 7.6 Hz, 1H). **ESI-MS:** 281.80 $[M]^+$, 283.75 $[M+2]^+$. **Purity** (UPLC): 99.64%.

**Step V:** Preparation of 6-bromo-N4-methylquinoline-3,4-diamine **6**.

6-bromo-N-methyl-3-nitroquinolin-4-amine **5** (4.0 g, 14.18 mmol) was dissolved in ethyl acetate (100 ml) and stannous chloride dihydrate (10.75 g, 56.7 mmol) was added in cooling. Reaction mixture was stirred for 4 h. at ambient temperature. After completion of reaction, reaction mixture was cooled and poured into ice cooled KOH solution (1N, 100 ml). The ethyl acetate layer was separated, washed with water and brine. The ethyl acetate layer was filtered, dried over sodium sulphate and evaporated to give crude compound. The pure compound **6** was obtained by column chromatography by using 1-5% methanol/DCM as mobile phase as dark brown oil. (3.1 g, Yield: 87%).

**$^1$H NMR** (DMSO-$d_6$, 400 MHz) δ ppm: 2.85 (d, *J* = 5.6 Hz, 3 H), 5.03 (q, *J* = 5.6 Hz, 1 H), 5.13 (s, 2 H), 7.43 (dd, $J_1$ = 8.8 Hz, $J_2$ = 2 Hz, 1 H), 7.67 (d, *J* = 8.8 Hz, 1 H), 8.22 (d, *J* = 2 Hz, 1 H), 8.37(s, 1 H). **ESI-MS:** 251.8 $[M]^+$. **Purity** (UPLC): 89.00 %.

**Step VI:** Preparation of 8-bromo-1-methyl-1,3-dihydro-2H-imidazo[4,5-c]quinolin-2-one **7**.

6-bromo-N4-methylquinoline-3, 4-diamine **6** (3.0 g, 11.90 mmol) was dissolved in DCM (30 ml) and triethylamine (3.61g, 35.7 mmol) was added. Reaction was cooled up to 0 $^oC$ using ice bath. Phosgene (20% in toluene) (3.53 g, 17.85 mmol) was added at 0 $^oC$. After stirring at 0 $^oC$ for 20 min., reaction was quenched using saturated $NaHCO_3$ solution, stirred for 5 min. The solution was extracted using DCM (2X50 ml). The organic layer was dried over sodium sulphate, filtered and evaporated to give crude compound. Crude product was

stirred in n-hexane (20 ml) and filtered to get product pure 8-bromo-1-methyl-1,3-dihydro-2H-imidazo[4,5-c]quinolin-2-one **7** as white solid (2.4 g, Yield: 72%).

**$^1$H NMR** (DMSO-$d_6$, 400 MHz) δ ppm: 3.79 (s, 1 H), 7.76 (dd, $J_1$ = *2 Hz*, $J_2$ = *8.8 Hz*, 1 H), 7.96 (d, *J = 9.2 Hz*, 1 H), 8.46 (d, *J = 1.6 Hz*, 2 H), 8.71 (s, 1 H), 11.67 (s, 1 H). **ESI-MS:** 277.8 $[M]^+$, 279.7 $[M+2]^+$. **Purity** (UPLC): 96.69 %.

**Step VI:** Preparation of **8a-g.**

A solution of 8-bromo-1-methyl-1,3-dihydro-2H-imidazo[4,5-c]quinolin-2-one **7** (1.04 mmol) in DMF (10 ml) was cooled to 0 $^oC$ and stirred for 15 min under nitrogen. NaH (1.56 mmol) was added and stirred for 20 min. till the solution turns dark brown. Substituted benzyl bromide or chloride (1.56 mmol) dissolved in DMF (1 ml) was added, slowly at 0$^oC$ and stirred for 45 min at same temperature. After completion of reaction, cold water was added and product was extracted using DCM (2 X 40 ml). The organic layer was dried over sodium sulphate and evaporated to afford desired compound. (Yield: 70-85 %).

### 2.1.3.2. Spectral data of intermediate 8a-g.

### 2-(4-((8-bromo-1-methyl-2-oxo-1,2-dihydro-3H-imidazo[4,5-c]quinolin-3-yl)methyl)phenyl) -2-methylpropanenitrile (8a)

**8a** was prepared following the general procedure described in section 2.1.3.1 (Step VII) as a white solid.

**$^1$H NMR** (DMSO-$d_6$, 400 MHz) δ ppm: 1.80 (s, 6H), 3.50 (s, 3H), 5.10 (s, 2H), 6.95 (m, 2H), 7.30 (dd, $J_1$ = 8.8 Hz, $J_2$ = 2.2 Hz, 2H), 7.70 (dd, $J_1$ = 8.8 Hz, $J_2$ = 2.2 Hz, 1H), 7.85 (d, *J* = 8.8 Hz 1H), 8.50 (s, 1H), 8.70 (s, 1H). **ESI-MS:** 435.3 $[M]^+$, 435.3 $[M+2]^+$. **Purity** (UPLC): 94.23%.

**8-bromo-3-(4-isopropylbenzyl)-1-methyl-1,3-dihydro-2H-imidazo[4,5-c]quinolin-2-one (8b)**

**8b** was prepared following the general procedure described in section 2.1.3.1 (Step VII) as a white solid.

**$^1$H NMR** (DMSO-$d_6$, 400 MHz) δ ppm: 1.20 (d, $J$ = 6.8 Hz, 6H), 2.40 (m, 1H), 3.55 (s, 3H), 5.12 (s, 2H), 6.90 (m, 2H), 7.38 (dd, $J_1$ = 8.8 Hz, $J_2$ = 2.2 Hz, 2H), 7.71 (dd, $J_1$ = 8.8 Hz, $J_2$ = 2.2 Hz, 1H), 7.80 (d, $J$ = 8.8 Hz,1H), 8.50 (s, 1H), 8.72 (s, 1H). **ESI-MS:** 410.2 $[M]^+$, 412.2 $[M+2]^+$. **Purity** (UPLC): 93.45 %.

**8-bromo-3-(4-methoxybenzyl)-1-methyl-1,3-dihydro-2H-imidazo[4,5-c]quinolin-2-one (8c)**

**8c** was prepared following the general procedure described in section 2.1.3.1 (Step VII) as off white solid.

**$^1$H NMR** (DMSO-$d_6$, 400 MHz) δ ppm: 3.70 (s, 3H), 3.86 (s, 3H), 5.18 (s, 2H), 6.89 (m, 2H), 7.36 (dd, $J_1$ = 8.8 Hz, $J_2$ = 2.0 Hz, 2H), 7.75 (dd, $J_1$ = 8.8 Hz, $J_2$ = 2.0 Hz, 1H), 7.95 (d, $J$ = 8.8 Hz, 1H), 8.47 (s, 1H), 8.88 (s, 1H). **ESI-MS:** 398.0 $[M]^+$, 400.0 $[M+2]^+$. **Purity** (UPLC): 93.85 %.

**8-bromo-1-methyl-3-(4-methylbenzyl)-1,3-dihydro-2H-imidazo[4,5-c]quinolin-2-one (8d)**

**8d** was prepared following the general procedure described in section 2.1.3.1 (Step VII) as a white solid.

**$^1$H NMR** (DMSO-$d_6$, 400 MHz) δ ppm: 2.20 (s, 3H), 3.53 (s, 3H), 5.15 (s, 2H), 6.88 (m, 2H), 7.38 (dd, $J_1$ = 8.8 Hz, $J_2$ = 2.2 Hz, 2H), 7.72 (dd, $J_1$ = 8.8 Hz, $J_2$ = 2.2 Hz, 1H), 7.90 (d, $J$ = 8.8 Hz, 1H), 8.48 (s, 1H), 8.82 (s, 1H). **ESI-MS:** 382.4 $[M]^+$, 384.4 $[M+2]^+$. **Purity** (UPLC): 92.21%.

**8-bromo-1-methyl-3-(4-nitrobenzyl)-1,3-dihydro-2H-imidazo[4,5-c]quinolin-2-one (8e)**

**8e** was prepared following the general procedure described in section 2.1.3.1 (Step VII) as a white solid.

**$^1$H NMR** (DMSO-$d_6$, 400 MHz) δ ppm: 3.80 (s, 3H), 5.30 (s, 2H), 7.10 (m, 2H), 7.68 (dd, $J_1$ = 8.8 Hz, $J_2$ = 2.0 Hz, 2H), 7.85 (dd, $J_1$ = 8.8 Hz, $J_2$ = 2.0 Hz, 1H), 8.10 (d, $J$ = 8.8 Hz, 1H), 8.55 (s, 1H), 8.90 (s, 1H). **ESI-MS:** 413.2 $[M]^+$, 415.3 $[M+2]^+$. **Purity** (UPLC): 96.41 %.

**8-bromo-3-(4-fluorobenzyl)-1-methyl-1,3-dihydro-2H-imidazo[4,5-c]quinolin-2-one (8f)**

**8f** was prepared following the general procedure described in section 2.1.3.1 (Step VII) as a white solid.

**$^1$H NMR** (DMSO-$d_6$, 400 MHz) δ ppm: 3.85 (s, 3H), 5.25 (s, 2H), 6.90 (m, 2H), 7.20 (m, 2H), 7.80 (m, 1H), 8.18 (m, 1H), 8.55 (s, 1H), 8.85 (s, 1H). **ESI-MS:** 386.2 $[M]^+$, 388.2 $[M+2]^+$. **Purity** (UPLC): 95.22%.

**3-benzyl-8-bromo-1-methyl-1,3-dihydro-2H-imidazo[4,5-c]quinolin-2-one (8g)**

**8g** was prepared following the general procedure described in section 2.1.3.1 (Step VII) as a white solid.

**$^1$H NMR** (DMSO-$d_6$, 400 MHz) δ ppm: 3.82 (s, 3H), 5.10 (s, 2H), 7.10 (m, 5H), 7.90 (dd, $J_1$ = 8.8 Hz, $J_2$ = 2.0 Hz, 1H), 8.20 (d, $J$ = 8.8 Hz, 1H), 8.55 (s, 1H), 8.90 (s, 1H). **ESI-MS:** 368.1 $[M]^+$, 370.2 $[M+2]^+$. **Purity** (UPLC): 96.17%.

**Step VIII:** Preparation of **9a-g** and **10a-m.**

A mixture of bromo quinoline **8a-j** (1.00 mmol) and bistriphenylphosphine palladium dichloride [$PdCl_2$ $(PPh_3)_2$] (0.01 mmol) in DMF (10 ml) was heated at 80-85 $^oC$ for 30 min, under Nitrogen atmosphere. To this mixture substituted boronic acid/ester (1.00 mmol) dissolved in DMF (9 ml) and (6.00 mmol) potassium bicarbonate ($KHCO_3$) (6.00 mmol) dissolved in water (10 ml) were added. The mixture was heated at 95 $^oC$ for 2 h. The mixture was cooled to 0-5 $^oC$; water (50ml) was added and stirred for 1 h. The crude product was filtered and washed with water, dried. Crude product was purified using flash chromatography using 0-10% MeOH in DCM mobile phase to give the titled compound. (Yield: 65-80 %).

### 2.1.3.3. Spectral data of final compounds 9a-g and 10a-m.

All final compounds were characterised using $^1H$ NMR, ESI-MS, and CHN analysis, melting point are also reported (uncorrected). Most potent compounds **9c** and **10h** were fully characterised using $^1H$ NMR, $^{13}C$ NMR, ESI-MS and IR. Purity of all compounds was checked using UPLC (ultra-performance liquid chromatography).

**2-methyl-2-(4-((1-methyl-2-oxo-8-(quinolin-3-yl)-1,2-dihydro-3H imidazo[4,5-c]quinolin-3-yl)methyl)phenyl)propanenitrile (9a)**

**9a** was prepared following the general procedure described in section 2.1.3.1 (Step VIII) as a white solid.

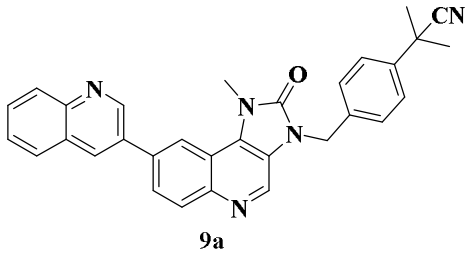


**9a**

**MP:** 210-211 $^{o}$C, **Yield:** 55%**.** **$^{1}$H NMR** (DMSO-$d_6$, 400 MHz) δ ppm: 1.80 (s, 6H), 3.82 (s, 3H), 5.21(s, 2H), 6.90 (d, *J* = 8.8 Hz, 2H), 7.34 (d, *J* = 8.4 Hz, 2H), 7.64-7.68 (m, 1H), 7.74-7.80 (m, 1H), 8.07-8.12 (m, 2H), 8.22 (s, 2H), 8.72 (s, 1 H), 8.82 (s, 1H), 8.94 (s, 1H), 9.05-9.10 (m, 1H). **Analysis (CHNS):** Calculated for $C_{31}H_{25}N_5O$: C, 77.00%; H, 5.21%; N, 14.48%; Found: C, 77.10%; H, 5.15%; N, 14.40%. **ESI-MS:** 484.5 $[M+H]^+$. **Purity** (UPLC): 99.69%.

**3-(4-isopropylbenzyl)-1-methyl-8-(quinolin-3-yl)-1,3-dihydro-2H-imidazo[4,5-c]quinolin-2-one (9b)**

**9b** was prepared following the general procedure described in section 2.1.3.1 (Step VIII) as a white solid.

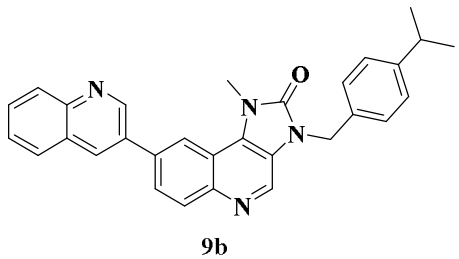


**9b**

**MP:** 205-206 $^{o}$C, **Yield:** 58%**.** **$^{1}$H NMR** (DMSO-$d_6$, 400 MHz) δ ppm: 1.22 (d, *J* = 6.8 Hz, 6H), 2.44 (m, 1H), 3.82 (s, 3H), 5.10 (s, 2H), 6.88 (d, *J* = 8.8 Hz, 2H), 7.32 (d, *J* = 8.4 Hz, 2H), 7.65-7.70 (m, 1H), 7.75-7.80 (m, 1H), 8.08-8.10 (m, 2H), 8.20 (s, 2H), 8.74 (s, 1H), 8.75 (s, 1H), 8.96 (s, 1H), 9.20 (d, *J* = 2.4 Hz, 1H). **Analysis (CHNS):** Calculated for $C_{30}H_{26}N_4O$: C, 78.58; H, 5.72; N,

12.22; Found: C, 78.65%; H, 5.78%; N, 12.18%. **ESI-MS:** 459.5 $[M+H]^+$. **Purity** (UPLC): 98.31%.

**3-(4-methoxybenzyl)-1-methyl-8-(quinolin-3-yl)-1,3-dihydro-2H-imidazo[4,5-c]quinolin-2-one (9c)**

**9c** was prepared following the general procedure described in section 2.1.3.1 (Step VIII) as a white solid.

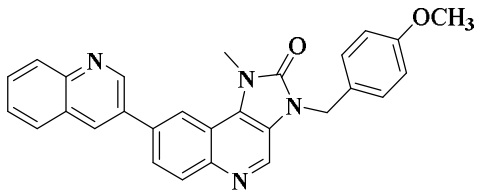


**9c**

**MP:** 215-216 $^oC$, **Yield:** 60%. **$^1$H NMR** (DMSO-$d_6$, 400 MHz) δ ppm: 3.71 (s, 3H), 4.04 (s, 3H), 5.22 (s, 2H), 6.92 (d, $J$ = 8.8 Hz, 2H), 7.38 (d, $J$ = 8.4 Hz, 2H), 7.67-7.71 (m, 1H), 7.79-7.83 (m, 1H), 8.09-8.13 (m, 2H), 8.17 (s, 2H), 8.75 (s, 1H), 8.87 (s, 1H), 8.90 (s, 1H), 9.47 (d, $J$ = 2.4 Hz, 1H). **$^{13}$C NMR** (100 MHz, DMSO-$d_6$): δ ppm: 30.76, 44.22, 55.50, 114.54, 116.17, 119.77, 119.68, 122.21, 127.54, 128.05, 128.93, 129.04, 129.09, 129.48, 130.21, 131.30, 132.68, 133.67, 133.95, 135.00, 144.01, 147.33, 150.16, 153.77, 159.24. **Analysis (CHNS):** Calculated for $C_{28}H_{22}N_4O_2$: C, 75.32; H, 4.97; N, 12.55; Found: C, 75.40%; H, 5.01%; N, 12.68%. **IR (KBr)** ν: 3404, 2918, 1712, 1697, 1514, 1342, 1246, 1178 cm-1. **ESI-MS:** 447.1 $[M+H]^+$. **Purity** (UPLC): 97.98%.

**1-methyl-3-(4-methylbenzyl)-8-(quinolin-3-yl)-1,3-dihydro-2H-imidazo[4,5-c]quinolin-2-one (9d)**

**9d** was prepared following the general procedure described in section 2.1.3.1 (Step VIII) as a white solid.

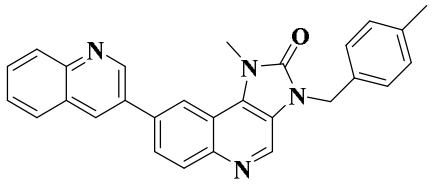

**9d**

**MP:** 198-199 $^{o}$C, **Yield:** 65%. **$^{1}$H NMR** (DMSO-$d_6$, 400 MHz) δ ppm: 2.15 (s, 3H), 3.65 (s, 3H), 5.18 (s, 2H), 6.90 (d, *J* = 8.8 Hz, 2H), 7.35 (d, *J* = 8.4 Hz, 2H), 7.66-7.68 (m, 1H), 7.70-7.77 (m, 1H), 8.12-8.18 (m, 2H), 8.21 (s, 2H), 8.75 (s, 1H), 8.80 (s, 1H), 8.88 (s, 1H), 9.22 (d, *J* = 2.4 Hz, 1H). **Analysis (CHNS):** Calculated for $C_{28}H_{22}N_4O$: C, 78.12; H, 5.15; N, 13.01; Found: C, 78.20; H, 5.25; N, 13.05. **ESI-MS:** 431.2 $[M+H]^+$. **Purity** (UPLC): 98.32%.

**1-methyl-3-(4-nitrobenzyl)-8-(quinolin-3-yl)-1,3-dihydro-2H-imidazo[4,5-c]quinolin-2-one (9e)**

**9e** was prepared following the general procedure described in section 2.1.3.1 (Step VIII) as a white solid.

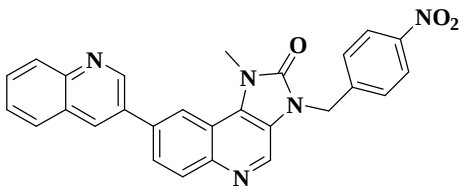

**9e**

**MP:** 221-222 $^{o}$C, **Yield:** 55%. **$^{1}$H NMR** (DMSO-$d_6$, 400 MHz) δ ppm: 3.71 (s, 3H), 5.35 (s, 2H), 7.20 (d, *J* = 8.8 Hz, 2H), 7.68 (d, *J* = 8.4 Hz, 2H), 7.68-7.72 (m, 1H), 7.84-7.90 (m, 1H), 8.10-8.15 (m, 2H), 8.20 (s, 2H), 8.72(s, 1H), 8.88 (s, 1H), 9.10 (s, 1H), 9.32 (d, *J* = 2.4 Hz, 1H). **Analysis (CHNS):** Calculated for $C_{27}H_{19}N_5O_3$: C, 70.27; H, 4.15; N, 15.18; Found: C, 70.32; H, 4.25; N, 15.25. **ESI-MS:** 462.2 $[M+H]^+$. **Purity** (UPLC): 98.48%.

**3-(4-fluorobenzyl)-1-methyl-8-(quinolin-3-yl)-1,3-dihydro-2H-imidazo[4,5-c]quinolin-2-one (9f)**

**9f** was prepared following the general procedure described in section 2.1.3.1 (Step VIII) as a white solid.

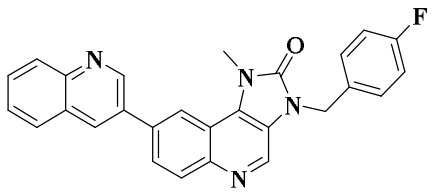

**9f**

**MP:** 208-209 $^{o}$C, **Yield:** 50%. **$^{1}$H NMR** (DMSO-$d_6$, 400 MHz) δ ppm: 3.65 (s, 3H), 5.26 (s, 2H), 7.19-7.23 (m, 2H), 7.38-7.42 (m, 2H), 7.68-7.73 (m, 1H), 7.79-7.84 (m, 1H), 8.03-8.10 (m, 3H), 8.16-8.18 (m, 1H), 8.25-8.18 (m, 1H), 8.45-8.46 (m, 1H), 9.03 (s, 1H), 9.10 (m, 1H). **Analysis (CHNS):** Calculated for $C_{27}H_{19}FN_4O$: C, 74.64; H, 4.41; F, 4.37; N, 12.90; Found: C, 74.72; H, 4.50; F, 4.44; N, 13.00. **ESI-MS:** 435.1 $[M+H]^+$. **Purity** (UPLC): 99.21%.

**3-benzyl-1-methyl-8-(quinolin-3-yl)-1,3-dihydro-2H-imidazo[4,5-c]quinolin-2-one (9g)**

**9g** was prepared following the general procedure described in section 2.1.3.1 (Step VIII) as a white solid.

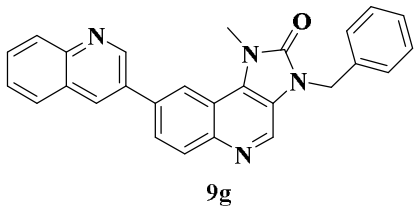

**9g**

**MP:** 194-195 $^{o}$C, **Yield:** 54%. **$^{1}$H NMR** (DMSO-$d_6$, 400 MHz) δ ppm: 3.66 (s, 3H), 5.28 (s, 2H), 7.36 (m, 4H), 7.38 (m, 1H), 7.66-7.70 (m, 1H), 7.77-7.81 (m,

1H), 8.20-8.15 (m, 2H), 8.35 (s, 2H), 8.72 (s, 1H), 8.82 (s, 1H), 9.05 (s, 1H), 9.35 (d, *J* = 2.4 Hz, 1 H). **Analysis (CHNS):** Calculated for $C_{27}H_{20}N_4O$: C, 77.87; H, 4.84; N, 13.45; Found: C, 77.95; H, 4.98; N, 13.49. **ESI-MS:** 417.20 $[M+H]^+$. **Purity** (UPLC): 97.13%.

**N-(6-(3-(4-methoxybenzyl)-1-methyl-2-oxo-2,3-dihydro-1H-imidazo[4,5-c]quinolin-8-yl)benzo[d]thiazol-2-yl)acetamide (10a)**

**10a** was prepared following the general procedure described in section 2.1.3.1 (Step VIII) as a white solid.

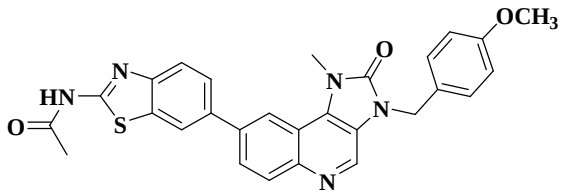


**10a**

**MP:** 245-246 $^oC$, **Yield:** 45%**.** **$^1$H NMR** (DMSO-$d_6$, 400 MHz) δ ppm: 2.23 (s, 3H), 3.71 (s, 3H), 4.00 (s, 3H), 5.21 (s, 2H), 6.90 (d, *J* = 8.8 Hz, 2H), 7.36 (d, *J* = 8.8 Hz, 2H), 7.86(d, *J* = 8.4 Hz, 1H), 7.95 (dd, $J_1$ = 1.6 Hz, $J_2$ = 8.4 Hz, 1H), 8.02 (dd, $J_1$ = 2.0 Hz, $J_2$ = 9.2 Hz, 1H), 8.10 (d, *J* = 8.8 Hz, 1H), 8.54 (s, 1H), 8.59 (s, 1H), 8.84 (s, 1H), 12.41(bs, 1H). **Analysis (CHNS):** Calculated for $C_{28}H_{23}N_5O_3S$: C, 66.00; H, 4.55; N, 13.74; S, 6.29; Found: C, 66.10; H, 4.61; N, 13.80; S, 6.25. **ESI-MS:** 510.0 $[M+H]^+$. **Purity** (UPLC): 98.82%.

**8-(2-aminobenzo[d]thiazol-6-yl)-3-(4-methoxybenzyl)-1-methyl-1,3-dihydro-2H-imidazo-[4,5-c]quinolin-2-one (10b)**

**10b** was prepared following the general procedure described in section 2.1.3.1 (Step VIII) as a white solid.

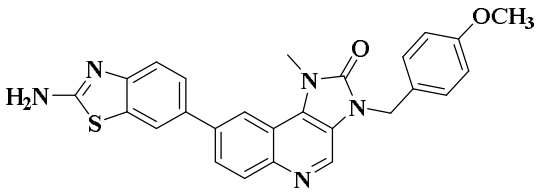

**10b**

**MP:** 255-256 $^{o}$C, **Yield:** 42%**. $^{1}$H NMR** (DMSO-$d_6$, 400 MHz) δ ppm: 3.70 (s, 3H), 3.99 (s, 3H), 5.02 (s, 2H), 6.90 (d, *J* = 8.4 Hz, 2H), 7.36 (d, *J* = 8.4 Hz, 2H), 7.45 (d, *J* = 8.4 Hz, 1H), 7.60 (s, 2H), 7.73 (d, *J* = 8.0 Hz, 1H), 7.96 (d, *J* = 8.8 Hz, 1H), 8.06 (d, *J* = 8.8 Hz, 1H), 8.24 (s, 1H), 8.51 (s, 1H), 8.82 (s, 1H). **Analysis (CHNS):** Calculated for $C_{26}H_{21}N_5O_2S$: C, 66.79; H, 4.53; N, 14.98; S, 6.86; Found: C, 66.90; H, 4.65; N, 15.15; S, 6.98. **ESI-MS:** 468.0 $[M+H]^+$. **Purity** (UPLC): 96.39%.

**3-(4-methoxybenzyl)-1-methyl-8-phenyl-1,3-dihydro-2H-imidazo[4,5-c]quinolin-2-one (10c)**

**10c** was prepared following the general procedure described in section 2.1.3.1 (Step VIII) as a white solid.

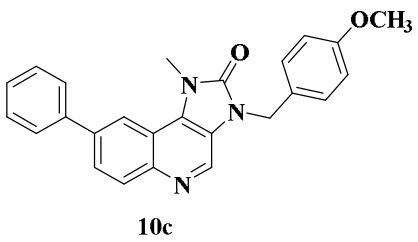

**10c**

**MP:** 185-186 $^{o}$C, **Yield:** 65%**. $^{1}$H NMR** (DMSO-$d_6$, 400 MHz) δ ppm: 3.62 (s, 3H), 3.95 (s, 3H), 5.18 (s, 2H), 6.95 (d, *J* = 8.4 Hz, 2H), 7.32 (d, *J* = 8.4 Hz, 2H), 7.45 (m, 4 H), 7.55-7.60 (m, 1H), 7.65 (d, *J = 8.0 Hz*, 1H), 7.92-7.94 (m, 1H), 8.10-8.15 (m, 1H), 8.82 (s, 1H). **Analysis (CHNS):** Calculated for

$C_{25}H_{21}N_3O_2$: C, 75.93; H, 5.35; N, 10.63; Found: C, 75.10; H, 5.45; N, 10.70. **ESI-MS:** 396.2 $[M+H]^+$. **Purity** (UPLC): 96.12%.

**3-(4-methoxybenzyl)-1-methyl-8-(pyridin-3-yl)-1,3-dihydro-2H-imidazo[4,5-c]quinolin-2-one (10d)**

**10d** was prepared following the general procedure described in section 2.1.3.1 (Step VIII) as a white solid.

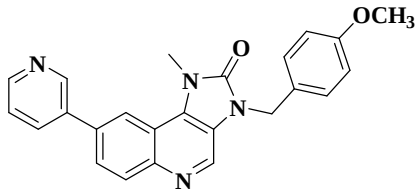


**10d**

**MP:** 214-215 $^oC$, **Yield:** 60%**.** **$^1$H NMR** (DMSO-$d_6$, 400 MHz) δ ppm: 3.68 (s, 3H), 3.85 (s, 3H), 5.18 (s, 2H), 6.85-6.90 (m, 2H), 6.95(d, $J$ = 8.8 Hz, 2H), 7.30-7.36 (m, 2H), 7.90-7.92 (m, 1H), 8.25-8.32 (m, 1H), 8.52 (m, 1H), 8.65-8.70 (m,1H), 8.71-8.78 (m, 1H), 8.88 (s, 1H). **Analysis (CHNS):** Calculated for $C_{24}H_{20}N_4O_2$: C, 72.71; H, 5.09; N, 14.13; Found: C, 72.88; H, 5.25; N, 14.25. **ESI-MS:** 397.2 $[M+H]^+$. **Purity** (UPLC): 97.12%.

**3-(4-methoxybenzyl)-8-(6-methoxypyridin-3-yl)-1-methyl-1,3-dihydro-2H-imidazo[4,5-c]quinolin-2-one (10e)**

**10e** was prepared following the general procedure described in section 2.1.3.1 (Step VIII) as a white solid.

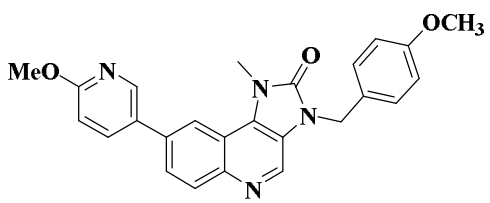


**10e**

**MP:** 224-225 $^{o}$C, **Yield:** 54%**. $^{1}$H NMR** (DMSO-$d_6$, 400 MHz) δ ppm: 3.65 (s, 3H), 3.93 (s, 3H), 3.98 (s, 3H), 5.20 (s, 2H), 6.89-6.92 (m, 2H), 6.97(d, *J* = 8.8 Hz, 2H), 7.34-7.36 (m, 2H), 7.94-7.97 (m, 1H), 8.22-8.25 (m, 1H), 8.51 (d, *J* = 2 Hz, 1H), 8.71 (d, *J* = 2 Hz, 1H), 8.85 (s, 1H). **Analysis (CHNS):** Calculated for $C_{25}H_{22}N_4O_3$: C, 70.41; H, 5.20; N, 13.14; Found: C, 70.55; H, 5.28; N, 13.25. **ESI-MS:** 427.1 $[M+H]^+$. **Purity** (UPLC): 97.60%.

**8-(6-methoxy-5-methylpyridin-3-yl)-3-(4-methoxybenzyl)-1-methyl-1,3-dihydro-2H-imidazo[4,5-c]quinolin-2-one (10f)**

**10f** was prepared following the general procedure described in section 2.1.3.1 (Step VIII) as a white solid.

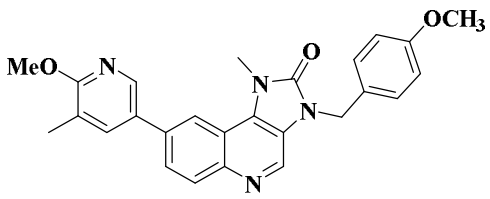


**10f**

**MP:** 212-213 $^{o}$C, **Yield:** 50%**. $^{1}$H NMR** (DMSO-$d_6$, 400 MHz) δ ppm: 2.40 (s, 3H), 3.60 (s, 3H), 3.85 (s, 3H), 3.90 (s, 3H), 5.22 (s, 2H), 6.60-6.70 (m, 2H), 7.10-7.20 (m, 2H), 7.55-7.65 (m, 1H), 8.02 (d, *J* = 8.8 Hz, 1H), 8.00-8.10 (m, 1H), 8.55 (d, J = 2 Hz, 1H), 8.70 (d, *J* = 2 Hz, 1H), 8.80 (s, 1H). **Analysis (CHNS):** Calculated for $C_{26}H_{24}N_4O_3$: C, 70.89; H, 5.49; N, 12.72; Found: C, 70.99; H, 5.55; N, 12.82. **ESI-MS:** 441.5 $[M+H]^+$. Purity (UPLC): 96.90%.

**8-(6-methoxy-5-(4H-1,2,4-triazol-4-yl)pyridin-3-yl)-3-(4-methoxybenzyl)-1-methyl-1,3-dihydro-2H-imidazo[4,5-c]quinolin-2-one (10g)**

**10g** was prepared following the general procedure described in section 2.1.3.1 (Step VIII) as a white solid.

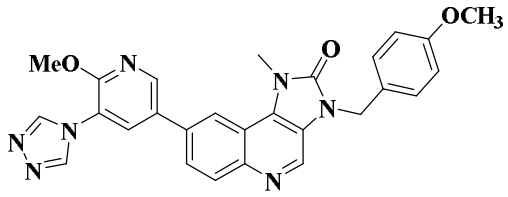


**10g**

**MP:** 233-234 $^{o}$C, **Yield:** 48%. **$^{1}$H NMR** (DMSO-$d_6$, 400 MHz) δ ppm: 3.70 (s, 3H), 3.99 (s, 3H), 4.03 (s, 3H), 5.21 (s, 2H), 6.89 (d, *J* = 8 Hz , 2H), 7.36 (d, *J* = 8 Hz, 2H), 8.07-8.08 (m, 1H), 8.11-8.13 (m, 1H), 8.55-8.56 (m, 1H), 8.58-8.59 (m, 2H), 8.83-8.87 (s, 1H), 9.01 (s, 2 H). **Analysis (CHNS):** Calculated for $C_{27}H_{23}N_7O_3$: C, 65.71; H, 4.70; N, 19.87; Found: C, 65.88; H, 4.80; N, 19.89. **ESI-MS:** 494.0 $[M+H]^+$. **Purity** (UPLC): 96.12%.

**N-(2-methoxy-5-(3-(4-methoxybenzyl)-1-methyl-2-oxo-2,3-dihydro-1H-imidazo[4,5-c]quinolin-8-yl)pyridin-3-yl)methanesulfonamide (10h)**

**10h** was prepared following the general procedure described in section 2.1.3.1 (Step VIII) as a white solid.

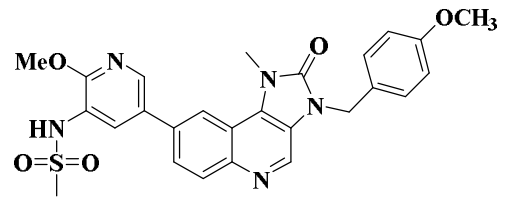


**10h**

**MP:** 225-226 $^{o}$C, **Yield:** 56%. **$^{1}$H NMR** (DMSO-$d_6$, 400 MHz) δ ppm: 3.11 (s, 3H), 3.70 (s, 3H), 3.97 (s, 3H), 3.99 (s, 3H), 5.20 (s, 2H), 6.90 (d, *J* = 8 Hz , 2H), 7.35 (d, *J* = 8 Hz , 2H), 7.90-7.92 (m, 1H), 8.05-8.10 (m, 2H), 8.49 (d, *J* = 2 Hz ,2H), 8.85 (s, 1H), 9.41 (s, 1H). **$^{13}$C NMR** (100 MHz, DMSO-$d_6$) δ: 30.59, 40.58, 44.18, 54.26, 55.49, 114.53, 116.16, 118.70, 121.85, 122.10, 126.09, 129.44, 129.79, 129.84, 131.17, 131.62, 133.65, 134.51, 141.64, 144.02, 153.75, 156.92, 159.22. **IR (KBr)** ν **cm$^{-1}$** = 3292, 1707, 1606, 1577, 1514,

1492, 1444, 1408, 1328, 1242, 1141, 827 cm-1. **Analysis (CHNS):** Calculated for $C_{26}H_{25}N_5O_5S$: C, 60.10; H, 4.85; N, 13.48; S, 6.17; Found: C, 60.14; H, 4.92; N, 13.55; S, 6.15. **ESI-MS:** 520.4 $[M+H]^+$. **Purity** (UPLC): 98.98%.

**N-(2-methoxy-5-(3-(4-methoxybenzyl)-1-methyl-2-oxo-2,3-dihydro-1H-imidazo[4,5-c]quinolin-8-yl)pyridin-3-yl)propane-2-sulfonamide (10i)**

**10i** was prepared following the general procedure described in section 2.1.3.1 (Step VIII) as a white solid.

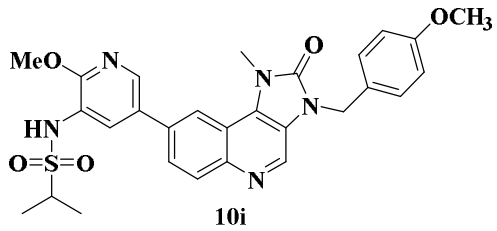


**10i**

**MP:** 236-237°C, **Yield:** 50%. **$^1$H NMR** (DMSO-$d_6$, 400 MHz) δ ppm: 1.8 (d, *J* = 6.8 Hz, 6H), 2.98-3.02 (m, 1H), 3.68 (s, 3H), 3.92 (s, 3H), 3.95 (s, 3H), 5.18 (s, 2H), 6.92 (d, *J* = 8 Hz , 2H), 7.34 (d, *J* = 8 Hz , 2H), 7.88-7.82 (m, 1H), 8.02-8.10 (m, 2H), 8.45 (d, *J* = 2 Hz ,1H), 8.52 (d, *J* = 2 Hz ,1H), 8.80 (s, 1H), 9.30 (s, 1H). **Analysis (CHNS):** Calculated for $C_{28}H_{29}N_5O_5S$: C, 61.41; H, 5.34; N, 12.79; S, 5.85; Found: C, 61.38; H, 5.24; N, 12.62; S, 5.72. **ESI-MS:** 548.4 $[M+H]^+$. **Purity** (UPLC): 99.30%.

**N-(2-methoxy-5-(3-(4-methoxybenzyl)-1-methyl-2-oxo-2,3-dihydro-1H-imidazo[4,5-c]quinolin-8-yl)pyridin-3-yl)cyclopropanesulfonamide (10j)**

**10j** was prepared following the general procedure described in section 2.1.3.1 (Step VIII) as a white solid.

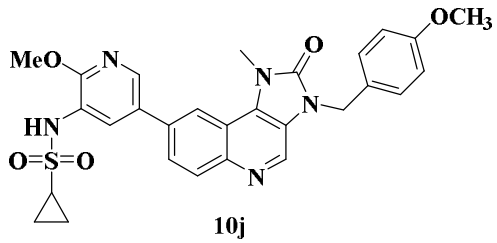


**10j**

**MP:** 230-231°C, **Yield:** 50%. **$^1$H NMR** (DMSO-$d^6$, 400 MHz) δ ppm: 1.12-1.14 (m, 2H), 1.28-1.30 (m, 2H), 1.98-2.05 (m, 1H), 3.68 (s, 3H), 3.96 (s, 3H), 3.98 (s, 3H), 5.18 (s, 2H), 6.92 (d, *J* = 8 Hz, 2H), 7.33 (d, *J* = 8 Hz, 2H), 7.88-7.85 (m, 1H), 8.02-8.10-8.20 (m, 2H), 8.44 (d, *J* = 2 Hz,1H), 8.52(d, *J* = 2 Hz, 1H), 8.82 (s, 1H), 9.38 (s, 1H). **Analysis (CHNS):** Calculated for $C_{28}H_{27}N_5O_5S$: C, 61.64; H, 4.99; N, 12.84; S, 5.88; Found: C, 61.78; H, 5.10; N, 12.94; S, 5.95. **ESI-MS:** 546.4 $[M+H]^+$. **Purity** (UPLC): 97.25%.

**N-(2-methoxy-5-(1-(4-methoxybenzyl)-3-methyl-2-oxo-2,3-dihydro-1H-imidazo[4,5-c]quinolin-8-yl)pyridin-3-yl)methanesulfonamide (10k)**

**10k** was prepared following the general procedure described in section 2.1.3.1 (Step VIII) as a white solid.

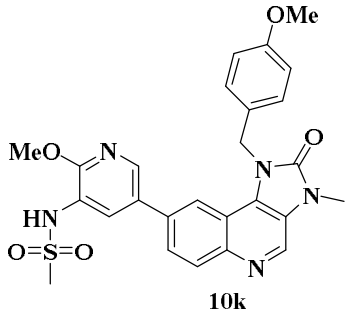


**10k**

**MP:** 220-221°C, **Yield:** 54%. **$^1$H NMR** (DMSO-$d_6$, 400 MHz) δ ppm: 3.10 (s, 3H), 3.63 (s, 3H), 3.63 (s, 3H), 3.99 (s, 3H), 5.59 (s, 2H), 6.89 (d, *J* = 8 Hz , 2H), 7.21 (d, *J* = 8 Hz , 2H), 7.84-7.87 (m, 2H), 8.07-8.13 (m, 2H), 8.24-8.25 (m, 1H), 8.86 (s, 1H), 9.42 (s, 1H). **Analysis (CHNS):** Calculated for

$C_{26}H_{25}N_5O_5S$. C, 60.10; H, 4.85; N, 13.48; S, 6.17; Found: C, 60.18; H, 5.00; N, 13.60; S, 6.26. **ESI-MS:** 520.0 $[M+H]^+$. **Purity (**UPLC): 98.32%.

**N-(2-methoxy-5-(3-(1-(4-methoxyphenyl)ethyl)-1-methyl-2-oxo-2,3-dihydro-1H-imidazo[4,5-c]quinolin-8-yl)pyridin-3-yl)methanesulfonamide (10l)**

**10l** was prepared following the general procedure described in section 2.1.3.1 (Step VIII) as a white solid.

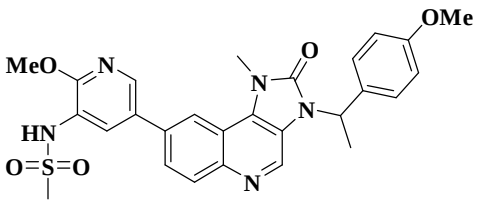


**10l**

**MP:** 242-243°C, **Yield:** 44%. **$^1$H NMR** (DMSO-$d_6$, 400 MHz) δ ppm: 1.92 (d, *J* = 4 Hz, 3H), 3.11 (s, 3H), 3.72 (s, 3 H), 3.97 (s, 3H), 4.00 (s, 3H), 5.84-5.85 (m, 1H), 6.91 (d, *J* = 8 Hz, 2H), 7.37 (d, *J* = 8 Hz, 2H), 7.90-7.92 (m, 1H), 8.04-8.07 (m, 2H), 8.49-8.54 (m, 2H), 8.58 (s, 1H), 9.41 (s, 1H). **Analysis (CHNS):** Calculated for $C_{27}H_{27}N_5O_5S$. C, 60.77; H, 5.10; N, 13.12; S, 6.01; Found: C, 60.88; H, 5.15; N, 13.20; S, 6.10. **ESI-MS:** 534.2 $[M+H]^+$. **Purity** (UPLC): 97.79%.

**N-(2-methoxy-5-(3-(4-methoxyphenethyl)-1-methyl-2-oxo-2,3-dihydro-1H-imidazo[4,5-c]quinolin-8-yl)pyridin-3-yl)methanesulfonamide (10m)**

**10m** was prepared following the general procedure described in section 2.1.3.1 (Step VIII) as a white solid.

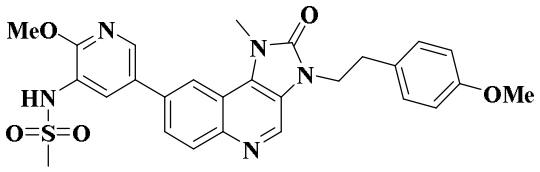

**10m**

**MP:** 249-250$^{o}$C, **Yield:** 40%. **$^{1}$H NMR** (DMSO-$d_6$, 400 MHz) δ ppm: 3.11 (s, 3H), 3.76 (s, 3H), 3.88 (s, 3H), 3.92 (s, 3H), 4.10 (t, *J* = 6.8 Hz, 2H ), 4.98 (t, *J* = 6.8 Hz, 2H), 6.85 (d, *J* = 8 Hz, 2H), 7.22 (d, *J* = 8 Hz, 2 H), 7.93-7.95 (m, 1H), 8.10-8.12 (m, 2H), 8.51-8.54 (m, 2H), 8.88 (s, 1H), 9.44 (s, 1H). **Analysis (CHNS):** Calculated for $C_{27}H_{27}N_5O_5S$. C, 60.77; H, 5.10; N, 13.12; S, 6.01; Found: C, 60.68; H, 5.08; N, 13.10; S, 5.92. **ESI-MS:** 534.2 $[M+H]^+$. **Purity** (UPLC): 98.51%.

### 2.1.4. Synthesis of N-(2-methoxy-5-(4,4,5,5-tetramethyl-1,3,2-dioxaborolan-2-yl)pyridin-3-yl)methanesulfonamide (16).

2-Methoxy-3-pyridyl boronate ester intermediate **16** was prepared using 5-bromo-3-nitropyridin-2-ol **11** which was reacted with $POCl_3$ to get chloro compound **12**. Chloro compound **12** was reacted with sodium methoxide in methanol to give 2-Methoxy-3-Nitro-5- pyridine **13**, Nitro group was reduce to amine compound **14** using iron followed by reacting with methane sulphonyl chloride to N-(5-bromo-2-methoxypyridin-3-yl)methanesulfonamide **15**. Bromo compound **15** was converted to pinacolto boronate ester using Miyaura Borylation Reaction using $PdCl_2$ (dppf) catalyst. Using similar condition various other boronate esters were synthesized (Scheme 2).

**Scheme 2**: Synthesis of N-(2-methoxy-5-(4,4,5,5-tetramethyl-1,3,2-dioxaborolan-2-yl)pyridin-3-yl)methanesulfonamide (16).

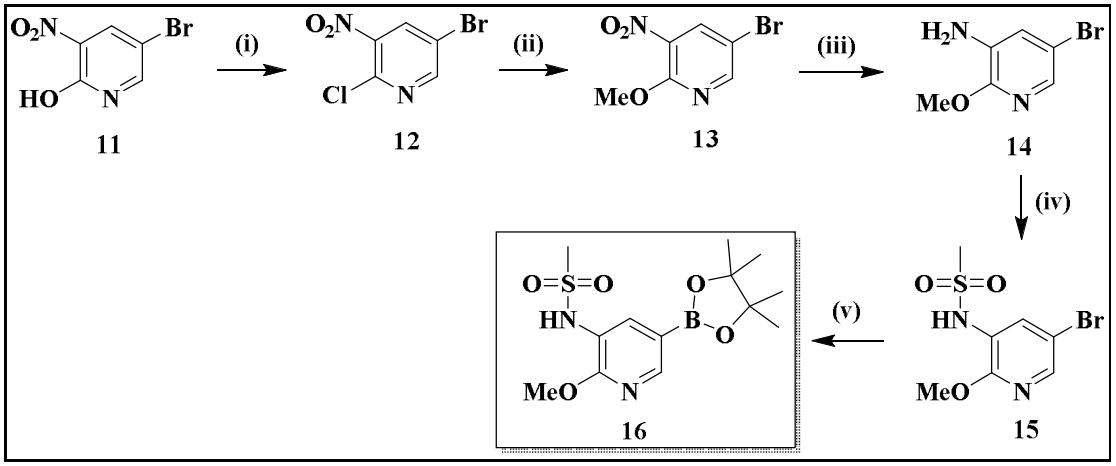


**Reagents and conditions:**(i) $POCl_3$, DIPEA, 80-85 $^oC$, 4 h; (ii) NaOMe, MeOH, 0-26 $^oC$, 4 h; (iii) Fe, Conc. HCl, EtOH, 26 $^oC$, 16 h; (iv) Mesyl-Chloride, Pyridine, 26 $^oC$, 24 h; (v) Bis(pinacolato)diboron, $PdCl_2$(dppf), (1,4)-Dioxane, Reflux, 24 h.

### 2.1.4.1. Experimental procedure N-(2-methoxy-5-(4,4,5,5-tetramethyl-1,3,2-dioxaborolan-2-yl)pyridin-3-yl)methanesulfonamide (16).

**Step I:** Preparation of 5-bromo-2-chloro-3-nitropyridine **12.**

5-bromo-3-nitropyridin-2-ol **11 (**10.0 g, 45.70 mmol) was suspended in $POCl_3$ (42.6 ml, 457.0 mmol). Reaction was cooled up to $0^oC$ and *N*,*N*-Diisopropylethylamine (DIPEA) (7.98 ml, 5.70 mmol) was added. The reaction mixture was heated to 80-85 $^oC$ for 4 h. Excess $POCl_3$ was distilled and cold water (100ml) was added. Solid formed was filtered to give 5-bromo-2-chloro-3-nitropyridine **12** as pale yellow solid (9.5 g, Yield: 88%), which was used for next reaction without further purification.

**Step II:** Preparation of 5-bromo-2-methoxy-3-nitropyridine **13.**

5-bromo-2-chloro-3-nitropyridine **12 (**9.0 g, 45.70 mmol) of was dissolved in methanol (50 ml). Reaction was cooled up to $0^oC$ using ice bath and NaOMe

(3.07 g, 56.9 mmol) dissolved in methanol (25 ml) was added. The reaction mixture was stirred for 4 h. at room temperature. Ice cold water (150 ml) was added. Solid formed was filtered to give 5-bromo-2-methoxy-3-nitropyridine **13** as off white solid (8.1 g, Yield: 92%).

**$^1$H NMR** (DMSO-$d_6$, 400 MHz) δ ppm: 4.02 (s, 3H), 8.69 (d, $J$ = 7.2 Hz, 2H). **ESI-MS:** 233.9 $[M+2]^+$. **Purity** (UPLC): 99.11%

**Step III:** Preparation of 5-bromo-2-methoxypyridin-3-amine **14.**

5-bromo-2-methoxy-3-nitropyridine **13 (**8.0 g, 34.3 mmol) was dissolved in ethanol (100 ml). Reaction was cooled up to 0 $^oC$ using ice bath and Iron (9.59 gm, 172 mmol) was added, followed by adding Conc. HCl. (10.43 ml). The reaction mixture was stirred for 16 h. at room temperature. Reaction mixture was filtered through hyflow. Excess of ethanol was evaporated, Sat. $NaHCO_3$ (100ml) and ethyl acetate (100ml) was added. Organic layer was separated, concentrated to give 5-bromo-2-methoxypyridin-3-amine **14** as thick oil (6.5 g, Yield: 93%).

**$^1$H NMR** (DMSO-$d_6$, 400 MHz) δ ppm: 3.85 (s, 3H), 5.30 (s, 2H), 6.99 (s, 1H), 7.39 (s, 1H). **HRMS:** 202.9781 $[M]^+$, 204.9773 $[M+2]^+$. **Purity** (UPLC): 98.01%.

**Step VI:** Preparation of N-(5-bromo-2-methoxypyridin-3-yl)methanesulfonamide **15.**

5-bromo-2-methoxypyridin-3-amine **14** (6.1 g, 30.0 mmol) of was dissolved in acetonitrile (10 ml) and pyridine (10 ml). Reaction was cooled up to 0$^oC$ using ice bath and methane sulfonyl chloride (4.13g, 36.1 mmol) was added. The reaction mixture was stirred for 24 h. at room temperature. Ice cold water (100 ml) was added. Solid formed was filtered to give N-(5-bromo-2-

methoxypyridin-3-yl)methanesulfonamide **15** as light yellow solid (6.5 g, Yield: 77%).

**$^1$H NMR** (DMSO-$d_6$, 400 MHz) δ ppm: 3.09 (s, 3H), 3.90 (s, 3H), 7.77 (s, 1H), 8.09 (s, 1H), 9.48 (s, 1H). **HRMS:** 280.9635 $[M]^+$, 282.9565 $[M+2]^+$. **Purity** (UPLC): 95.78%.

**Step VI:** Preparation of N-(2-methoxy-5-(4,4,5,5-tetramethyl-1,3,2-dioxaborolan-2-yl)pyridin-3-yl)methanesulfonamide **16.**

N-(5-bromo-2-methoxypyridin-3-yl)methanesulfonamide **15** (5.5 g, 19.56 mmol) was dissolved in 1,4-Dioxane (100 ml) under nitrogen. Bis (pinacolato) diboron (5.46 g, 21.52 mmol), [1,1'-Bis(diphenylphosphino)ferrocene]palladium(II) dichloride [PdCl2(dppf)] (0.716 g, 0.978 mmol) and Potassium acetate (5.76 g, 58.7 mmol) were added sequentially. The reaction mixture was refluxed for 24 h. 1,4-Dioxan was distilled out, to give crude product. Crude product was purified using column chromatography using Ethyl acetate: n-Hexane mobile phase to give N-(2-methoxy-5-(4,4,5,5-tetramethyl-1,3,2-dioxaborolan-2-yl)pyridin-3-yl)methanesulfonamide **16** as off white solid (5 g, Yield: 78%).

**$^1$H NMR** (DMSO-$d_6$, 400 MHz) δ ppm: 1.29 (s, 12H), 3.00 (s, 3H), 3.94 (s, 3H), 7.77 (s, 1H), 8.20 (s, 1H), 9.24 (s, 1H). **ESI-MS:** 328.7 $[M+H]^+$. **Purity** (UPLC): 95.54%.

Using scheme 1, total 20 compounds **9a-g** and **10a-m** were prepared, which were subjected for *in vitro* PI3Kδ inhibitory activity screening. Detailed assay protocol and PI3Kδ inhibitory activity data has been described in the next section.

## 2.2. Biological evaluation

As described earlier we have synthesised overall 20 compounds in imidazo-quinoline series. All the synthesized compounds were assessed for their PI3Kδ inhibitory activities in order to establish Structure Activity Relationship (SAR). Most potent compounds from this series were subjected for *in vitro* selectivity over related PI3K enzymes (α, β & γ) and mTOR. Potent and selective compounds were further subjected for *in vivo* anti-inflammatory and anti-cancer activities. Short listed compounds were also subjected for PK studies. Some additional profiling studies such as CYP inhibition study (*in vitro*), and hERG inhibition (Rb efflux assay) were conducted for the short listed compounds. Compound **9c**, **10h** and **10k** compounds were docked in the PI3Kδ ATP binding pocket to understand orientation and interactions with PI3K enzyme. The detailed assay protocols for various biological studies have been described below.

### 2.2.1. *In vitro* PI3K inhibitory activity assay

PI3K kinase activity assay kit (from Millipore) was used to screen the novel inhibitors. The assay was carried out according to the procedures suggested by the manufacturers. Briefly, the kinase reaction was setup with 25 ng of the enzyme (α or β or γ or δ PI3K enzyme), 10 µM PIP2 substrate and 1X kinase reaction buffer in 25 µL of volume per well. Different concentrations of test compounds were added to the reaction mixture and incubated for 1 h at 37 $^{o}$C. 25 µL/well of Biotinylated-$PIP_3$/EDTA working solution was added to the reaction well followed by 50 µl of GRP1 working solution to all wells. The reaction mixture was incubated for 1 h at 26 $^{o}$C and washed 4 times with 200µL/well 1X TBST (Tris-buffered saline with 0.1% Tween® 20). SA-HRP (Streptavidin-Horseradish Peroxidase) working solution (50 µl) was added and

again incubated at 26 $^{o}$C for 1 h. 100 µL of the Substrate TMB was added to develop the colour in the dark for 5-20 minutes and stopped by adding 100 µL of the stop solution. The absorbance was read at 450 nm and relative percentage of inhibition was calculated with respect to the positive control Biotinylated-$PIP_3$. Data was analysed and inhibition was calculated at the specified compound concentration under investigation **[73]**.

### 2.2.2. *In vivo* efficacy studies

The animal experiments were carried out on rat or mice, bred in-house. Animals were housed in groups of 6 animals per cage, for a week, in order to habituate them to vivarium conditions (25 ± 4 $^{o}$C, 60-65 % relative humidity, 12: 12 h light: dark cycle, with lights on at 7.30 am). All the animal experiments were carried out according to the internationally valid guidelines following approval by the 'Zydus Research Center animal ethical committee'.

### 2.2.3. Mouse xenograft model to test anti-tumor activity of test compounds

Male SCID mice were inoculated subcutaneously with 10 × 106 TMD-8 cells in 0.1 mL of PBS to the right flank **[74]**. Animals were observed twice weekly for occurrence of tumor. Once the tumors became palpable (around 100 $mm^3$) around 14 days after injection, mice were randomized into four groups (8-10 mice/group) in each study. Treatment with test compound **10h** (doses 3, 10 and 30 mg/kg), was initiated via oral route, once daily for 21 consecutive days. Tumor volume was determined every alternate day using digital callipers and the tumor volume was calculated using the formula: [length/2] × [width2]. Body weights of the animals were also recorded 3 times a week as a measure of treatment related side effect. Inhibition of tumor volume compared to vehicle control was considered as efficacy endpoint. Data were

expressed as mean ± SEM, and differences were considered statistically significant at $P < 0.05$ by Student t test.

### 2.2.4. Protocol for collagen induced arthritis (CIA) study in mice

CIA study is a representative animal model of human rheumatoid arthritis **[75]**. Following 7 days acclimation, male DBA1j (8 to 12-weeks old) mice were randomly assigned to groups according body weight. Mice were immunized subcutaneously in the tail using bovine type II collagen mix in complete Freund's adjuvant (CFA). Twenty-one days after the first immunization, mice were given booster dose of collagen in incomplete Freund's adjuvant (IFA). Mice were monitored every other day after the booster dose for the development of arthritis. Mice were recruited for the study once clinical signs were visible. Eight animals were assigned in each of the four groups [vehicle, positive control (NVP BEZ-235) and two doses of test compound, **10h**] and treatment was continued for two weeks and percentage inhibition in clinical score was recorded as per graded score. Body weights of the animals were also recorded 3 times a week as a measure of treatment related side effect and paw thickness measured twice a week. The mice were scored in a blinded manner (0–12) for signs of arthritis in each paw according to the following scale: 0 - no swelling or redness/normal paw; 1- swelling and/or redness in one digit; 2- swelling and/or redness in two or more digits; and 3- entire paw is swollen or red. The severity score was reported as the sum of all four paws for each mouse and severity was expressed as the average severity score for each group **[76]**.

### 2.2.5. Protocol for pharmacokinetic (PK) studies

A comparative single dose (3 mg/kg, po and 1 mg/kg, iv) PK profile of compounds **9c**, **10h** and Dactolisib was evaluated in overnight fasted

male C57BL/6J mice (n =6). Serial blood samples were collected in micro centrifuge tubes containing EDTA at pre-dose, 0.15, 0.3, 0.5, 0.75, 1, 2, 4, 6, 8, 24 and 30 h post-dose after compounds administration. Approximately 0.3 ml of blood was collected at each time point and centrifuged at 4$^{o}$C The obtained plasma was frozen, stored at-70 $^{o}$C and the concentrations of compounds in plasma were determined by the LC-MS/MS (Shimadzu LC10AD, USA), using YMC hydrosphere C18 (2.0 x 50 mm, 3 μm) column (YMC Inc., USA). The pharmacokinetic parameters, such as Tmax, $t_{1/2}$, Cmax, AUC and %F were calculated using a non-compartmental model of WinNonlin software version 5.2.1.

### 2.2.6. Protocol for safety pharmacology (toxicity) study

Repeated dose toxicity studies (14 days) of compounds were carried out in male wistar rats (WR). Briefly, animals were divided into three groups (n=9), a control group and separate groups for test compounds. To each of the test groups, a daily oral dose of compound **10h** was administered, twice a day (bid), under fasted conditions for 14 days. After completion of the treatment period (14 days), animals were sacrificed and subjected to a complete necropsy examination and also changes in toxicological parameters, such as gross pathology, clinical signs, body weight, organ weights and serum chemistry/ hematological changes were recorded.

### 2.2.7. *In vitro* CYP inhibition study assay

For CYP1A2, CYP2C8, CYP2C9, CYP2D6, CYP2C19 and CYP3A4 inhibition studies, Human liver microsomes (0.2 mg/ml), Testosterone (50 μM) / Dextromethorphan (5 μM) respectively, as probe substrates, potassium phosphate buffer (0.1 M; pH 7.4) and NADPH (1μM) were incubated

with different concentrations of test compounds (@1, 10 and 100 µM concentrations) at 37 $^{o}$C for 10 min, enzyme activity (% of control) was determined and $IC_{50}$ values were calculated **[77]**.

### 2.2.8. hERG inhibition

CHO (CHO-K1) cells stably expressing the hERG potassium channel were constructed and maintained in alpha-minimum essential medium (MEM) containing 10% fetal bovine serum, 1% penicillin-streptomycin, and 1% Geneticin in a humidified atmosphere at 37 $^{o}$C, with 5% $CO_2$. On the day before experiments, stable clones were seeded at 6 X 104 cells/well, in 96-well Plate and cultured for 24 h. In this assay, Rubidium (Rb) acts as a tracer for Potassium (K) movement across the cell membrane. The culture medium was exchanged to Rb loading medium and incubated for 1.5 h. Medium was discarded, the plate was washed with pH 7.3 buffer, and high $K^+$ buffer (pH = 7.3) containing compound **10h** was added to initiate the Rb efflux through the potassium channel. After 10 min. incubation, the supernatant was transferred to a new plate (Plate [A] 0. The plate containing the cells was lysed with 1% Triton-X 100 in pH 7.3 buffer (Plate [B]). Rb in Plates (A) and (B) was detected using an Ion Channel Reader 8000 (Aurora Biomed Inc.), and the Rb efflux rate (RE) and the efflux inhibition rate were calculated using the following equations [**78]**:

Rb efflux rate (RE) (%) = remained Rb (B)/total Rb (A+B) X 100

Efflux inhibition (%) = RE (test compound)

- RE (vehicle) / RE (positive control)
- RE (vehicle) X 100

### 2.2.9. Anti-proliferative assay

TMD8 cells were grown in RPMI-1640 with 10% FBS and supplemented with 55 μmol/L β-mercapto ethanol (β-ME). For Anti-proliferative assay, defined numbers of cells were incubated in 96 well plates with increasing concentration of **10h**, formulated in 100% DMSO (final concentration of DMSO in the well is 0.2%) for 96 hours. Cell growth was measured using MTT assay.

### 2.2.10. Docking protocol

To explain the selective PI3Kδ inhibitory activity of novel compounds, docking studies were carried out using Glide 5.6,1 the automated docking program implemented in the Schrodinger package. The geometry of compounds to be docked were subsequently optimized using the LigPrep version 2.6.2 The scoring function, binding mode and H-bonds were used to assess the binding affinity of the compounds. The PI3Kδ crystal structure complexed with INK-666 was retrieved from the RCSB Protein Data Bank (PDB entry **2WXK**). The active site was defined to include residues within 10 $A^0$ to any of the INK-666 atoms **[79]**.

## 2.3. Result and Discussion

In this section, we summarized results and discussion of imidazo-quinoline PI3Kδ inhibitors:

- *In vitro* PI3Kδ inhibitory activity, isoform selectivity and SAR
- *In vitro* CYP inhibition study, hERG liabilities and anti-proliferative activities
- *In vivo* anti-inflammatory activity in CIA mice model

- *In vivo* anti-tumor activity in mice xenograft model
- Pharmacokinetic (PK) studies of selected compounds in mice
- Safety pharmacology study in rat
- Docking studies to understand key interaction of potent compounds with PI3Kδ crystal structure

### 2.3.1. *In vitro* PI3Kδ inhibitory activity, selectivity and structure activity relationship (SAR)

Idelalisib and Dactolisib were employed as the positive control in *in vitro* studies. In Set-1 **[9a-g, Table 6]** it was found that the majority of 4-substituted-(benzyl)-8-quinolinyl-imidazo[4,5-c]quinolinone (**9a-g**) analogues displayed varying degree of PI3Kδ inhibitory activities at 100 nM concentration. The initial Compound **9a** bearing a 2-methyl-propanenitrile substitution on a benzyl ring showed moderate PI3Kδ inhibitory activity (56% PI3Kδ inhibition at 100 nM), while replacement of the nitrile group (compound **9b**: 73% inhibition) afforded enhanced PI3Kδ inhibitory activity, with an $IC_{50}$ value of 28.3 nM. Replacement of isopropyl group (**9b**) with methoxy group (**9c**, $IC_{50}$: 9.5 nM) and methyl group (**9d**, $IC_{50}$: 18.4 nM) led to higher PI3Kδ inhibitory activity, whereas replacement with the electron withdrawing nitro group (**9e**, 62% inhibition), electronegative Fluoro group (**9f**: 51% inhibition) and the unsubstituted compound **9g** (22% inhibition) showed weaker PI3Kδ inhibitory activity.

**Table 6:** *In vitro* PI3Kδ inhibitory activity data of Imidazo-quinoline derivatives with modification at $\mathbf{R_1}$ position (Set-1)

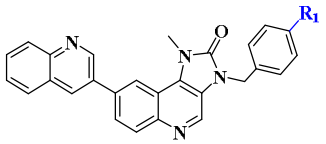

**9a-g**

| Comp. | $R_1$ | PI3Kδinhibition (%)[a, b] | PI3Kδ $IC_{50}$ (nM)[c] |
|---|---|---|---|
| **9a** |  | 56 | ND |
| **9b** |  | 73 | 28.3 |
| **9c** |  | **98** | **9.5** |
| **9d** | -$CH_3$ | 80 | 18.4 |
| **9e** | -$NO_2$ | 62 | ND |
| **9f** | -F | 51 | ND |
| **9g** | -H | 22 | ND |
| **Dactolisib** | - | 92 | 8 |
| **Idelalisib** | - | 96 | 2.1 |

[a]All the data are shown as the mean for at least two experiments. [b]PI3Kδ inhibition at the concentration of 100 nM using PI3K Kinase Activity/Inhibitor assay Kit from Millipore. [c]The $IC_{50}$ values for PI3Kδinhibition. ND: not detected

In Set-1, compound **9c** bearing methoxy group afforded the most potent PI3Kδ inhibitory activity, which was found to be similar to Dactolisib; $IC_{50}$:8 nM, **Table 6** and approximately 4.5 fold less potent compared to Idelalisib ($IC_{50}$: 2.1 nM). Thus, in the Set-1, reversing the positions of methyl ($N^1$ to $N^3$) and phenyl ($N^3$ to $N^1$) groups and introduction of carbon spacer (phenyl to benzyl) at $N^3$ position, followed by substitution of *p*-position of benzyl ring led to the single digit nM potent compound (**9c**), compound **9c** was evaluated for selectivity against PI3K isoforms (α, β, γ, δ) and m-TOR. In isoform selectivity assay, **9c** (PI3K; $IC_{50}$ α: 421 nM, β: 342 nM, γ: 38 nM and δ: 9.5 nM) showed moderate isoform selectivity, **Table 8.**

Further to improve PI3Kδ isoform selectivity, modelling studies were carried out, considering compound **9c** as primary lead. In Set-2, various substitutions were carried out on the 8th position of **9c** and favourable interactions of *p*-methoxy-benzyl substituted imidazo-quinoline ring with the key residues of selectivity pockets ($Trp_{760}$ in PI3Kδ) were assessed to improve PI3K*δ* isoform selectivity. Modelling study suggested that suitable substitution on the 8th position of compound **9c**, which favours to adopt the distorted propeller shape when bound to enzyme, could be responsible for PI3K*δ* selectivity. Based on these encouraging results of modelling study, ten compounds (**10a-m**) were designed in Set-2, **Table 7** and subjected for *in vitro* screening and their respective results are as follows.

**Table 7:** Influence of modification at **$R_2$** position of quinoline moiety on PI3Kδ inhibitory activity and isoform selectivity (Set-2)

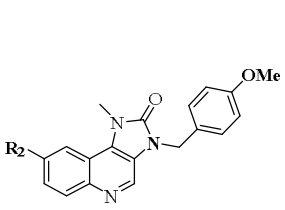


**10a-j**

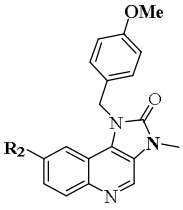


**10k**

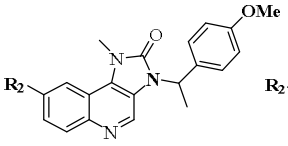


**10l**

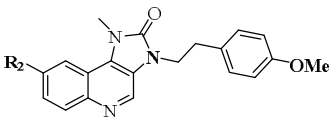


**10m**

| Comp. | $R_2$ | PI3Kδinhibition (%)[a,b] | PI3Kδ $IC_{50}$ (nM)[c] | Comp. | $R_2$ | PI3Kδinhibition (%)[a,b] | PI3Kδ $IC_{50}$ (nM)[c] |
|---|---|---|---|---|---|---|---|
| **10a** | 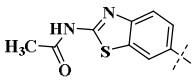 | 52 | ND | **10h** | 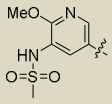 | **99** | **1.9** |
| **10b** | 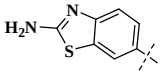 | 58 | ND | **10i** |  | 91 | 6.2 |
| **10c** |  | 72 | 29.4 | **10j** | 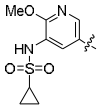 | 93 | 5.9 |
| **10d** |  | 81 | 20 | **10k** | 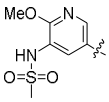 | 98 | 4.1 |

| | | | | | | | |
|---|---|---|---|---|---|---|---|
| **10e** | 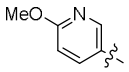 | 87 | 11.4 | **10l** | 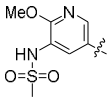 | 60 | ND |
| **10f** | 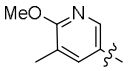 | 88 | 11.1 | **10m** | 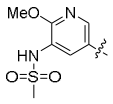 | 56 | ND |
| **10g** | 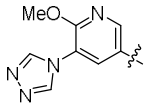 | 62 | ND | | **Idelalisib** | 96 | 2.1 |

[a]All the data are shown as the mean for at least two experiments. [b]PI3Kδ inhibition at the concentration of 100 nM using PI3K Kinase Activity/Inhibitor assay Kit from Millipore. [c]The $IC_{50}$ values for PI3Kδ inhibition.ND: not detected.

In the second set, we found that the PI3K*δ* inhibitory activity could be preserved to a large extent by making modifications at 8$^{th}$ position of quinoline in **9c**. As listed in Table 5 (Compounds **10a-m**), replacement of quinoline moiety in **9c** with benzthiazole (**10a** and **10b** (acylated **10a**)) displayed around 50% PI3Kδ inhibition at 100 nM. Phenyl derivative (**10c**) was found to be less potent (PI3K*δ* $IC_{50}$: 29.4 nM) compared to **9c**, while Pyridyl derivatives (**10d**) showed some improvement in the potency ($IC_{50}$: 20 nM). Introduction of methoxy (**10e**) and 3-methyl-2-methoxy substituents (**10f**)were found to be equipotent ($IC_{50}$: ~11 nM). Triazole motif (**10g**) showed less activity compared to **9c**, while *m*-methanesulfonamide derivative (**10h**) was found to be the most potent ($IC_{50}$: 1.9 nM) among all, presumably due favourable orientation and interactions in the affinity pocket and hinge regions. Replacement of methyl group in **10h**, with iso-propyl (**10i**) and cyclo-propyl (**10j**) showed three fold less activity compared to **10h**.

Interchanging the substitution in **10h** on imidazole ring (methyl at $N^3$ and para-methoxy benzyl at $N^1$, **10k**), found to be two fold less active compared to **10h**, suggesting that introduction of higher alkyl chain at $N^3$ destabilize favourable interactions with the key residues of hydrophobic region

and affinity pocket of PI3Kδ enzyme. Similarly, racemic compound **10l**, and **10m** (one carbon homologs at $N^3$ with respect to **10h**) were found to be less active.

### 2.3.2. Isoform selectivity study of 9c, 10h and 10k

Based on the above preliminary PI3Kδ inhibitory activity results, most potent compounds (**9c**, **10h** and **10k**) were evaluated for their selectivity against PI3K isoforms (α, β and γ) and mTOR. As shown in **Table 8**, Initial hit **9c** and **10k** showed moderate selectivity against other three PI3K isoforms and mTOR over PI3Kδ. Compound **10h** ($IC_{50}$: 1.9 nM) demonstrated 469, 310, 59 and >500 fold selectivity over PI3Kα, β, γ and m-TOR respectively. Moreover, it was noted that selectivity of **10h** against all the three isoforms was higher than standard compounds. In general, it was observed that the potency and selectivity of imidazo-quinoline based PI3Kδ inhibitors can be modulated using suitable substituents at $R^1$ and $R^2$ position.

**Table 8:** Isoform selectivity of compounds against PI3K (α,β,γ, and δ) and mTOR activities

| Comp. | Biochemical $IC_{50}$ [nM][a] | | | | |
|---|---|---|---|---|---|
| | PI3Kα[b] | PI3Kβ[b] | PI3Kγ[b] | PI3Kδ[b] | mTOR[b] (p70S6K) |
| **9c** | 421 | 342 | 38 | 9.5 | 676 |
| **10h** | **891** | **589** | **112** | **1.9** | **>1000** |
| **10k** | 289 | 241 | 42 | 4.1 | 580 |
| **Dactolisib** | 5 | 79 | 6 | 8 | 14 |
| **Idelalisib** | 831 | 571 | 92 | 2.1 | >1000 |

[a]The $IC_{50}$ values are shown as the mean for at least two experiments.[b]PI3K inhibitory activity assay Kit (Millipore) was used to screen the test compounds.

Highly potent and selective PI3Kδ inhibitor (**10h)** was selected for *in vitro* kinase profiling study at1 μM concentration, against 140 kinases and percent inhibition was found to <20% at 1 μM concentration, with **10h** across 140 kinase profiling panel.

### 2.3.3. Anti-proliferative activities, CYP (Cytochrome) inhibition and hERG (human ether-a-go-go-related gene) liabilities for Compound 10h

Compound **10h** was tested for its anti-proliferative activities against TMD-8 cell lines with Idelalisib as a reference compound. In anti-proliferative in vitro assay, **10h** and Idelalisib exhibited potent anti-proliferative activity with an $IC_{50}$ value of 340 and 795 nM respectively.

Additional profiling studies of compound **10h** was carried out and it was found to be devoid of CYP (<10% CYP inhibition at 10 μM concentration, for CYP1A2, CYP2C8, CYP2C9, CYP2D6, CYP2C19 and CYP3A4) and hERG liabilities ($IC_{50}$: > 30 μM), while Idelalisib showed moderate CYP3A4 68% inhibition **[57]**.

### 2.3.4. *In vivo* pharmacokinetic (PK) and pharmacodynamics (PD) studies of compound 10h

A comparative single dose (3 mg/kg, po and 1 mg/kg, iv) PK profile of compounds **9h**, **10h** and Dactolisib were evaluated in male C57BL/6J mice (n =6) and the various PK parameters (Tmax, Cmax, $t_{1/2}$, Cl, AUC and %F) were recorded **[Table 9]**. In PK study, **9c** showed moderate AUC, high clearance, this resulted into overall low bioavailability (~15%). Compound **10h** showed rapid Tmax, higher AUC (~5 fold, compared to standard), extended $t_{1/2}$ (~3.5 h) and good oral bioavailability (%F ~69 over standard, 38%). Compound

**10h** showed extended $t_{1/2}$ and higher AUC, which could be due to its low clearance compared to standard (8.24 vs 72.5 ml/min/kg, iv).

**Table 9:** Pharmacokinetic study parameters of **9c**, **10h** and **Dactolisib** in C57 mice

| Compd | Tmax (h) | Cmax (μg/ml) | $t_{1/2}$ (h) | Cl (ml/min/kg), iv | AUC (0-α) h μg/ml | %F* |
|---|---|---|---|---|---|---|
| **9c** | 0.38 | 127.61 | 2.31 | 22.9 | 329.08 | 14.77 |
| **10h** | 0.25 | 1278.49 | 3.48 | 8.24 | 3831.48 | 68.91 |
| **Dactolisib** | 0.21 | 273.83 | 1.88 | 72.5 | 243.64 | 37.82 |

[a]In male C57BL/6J mice (n=6), compounds were administered orally (p.o) at 3 mg/kgdose and plasma concentration was analysed by LC-MS, values indicate Mean ± SD.* Oral bioavailability (%F) was calculatewrt to iv AUC. Compounds **9c**, **10h** and Dactolisib administered at 1 mg/kg dose, iv AUC: 742.56, 1852.95 and 215.14 respectively.

Considering low bioavailability of **9c**, in PK study, only **10h** was evaluated. Collagen Induced Arthritis (CIA) mice model was used to assess anti-arthritic efficacy of test compounds. As described in the experimental section, Arthritis was developed in male DBA1j mice, using collagen mixture and mice were recruited for the study once clinical signs were visible. Eight animals were assigned in each of the four groups [vehicle, positive control (Dactolisib, 60 mg/kg) and two doses of test compound **10h** (10 and 30 mg/kg)]. Treatment was continued for four weeks and percentage inhibition in clinical score is recorded. As shown in the **Figure 22**, standard and **10h** showed significant reduction in the arthritic score, compared to vehicle control (untreated group).Two fold higher dose of a standard compound was used, considering two fold differences in the mice oral bioavailability. At 30 mg/kg

dose, compound **10h** showed superior activity compared to standard compound (dose 60 mg/kg). Body weights of the animals were also recorded 3 times a week as a measure of treatment related side effect and **10h** showed no significant reduction in the body weight, even at 30 mg/kg dose, while Dactolisib exhibited reduction in body weight.

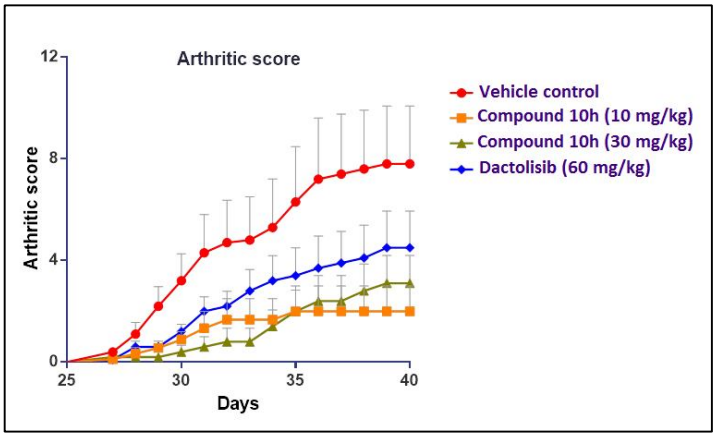


**Figure 22:** Effect of Compound **10h** and **Dactolisib** in CIA mice model

*In vivo* anti-tumor activity of **10h** was checked in male SCID mice xenograft model (inoculated with TMD-8 cells). Inhibition of tumor volume compared to vehicle control (untreated group) was considered as efficacy end point. As shown in **Figure 23**, three doses (3, 10 and 30 mg/kg/day, orally for 21 days) of **10h** were administered and it showed dose dependent reduction in the tumor volume. At 30 mg/kg dose, 10h showed complete inhibition of tumor volume compared to vehicle control. Body weights of the animals were also recorded and **10h** showed no significant reduction in the body weight, even at 30 mg/kg dose. Thus improved PK of **10h** justifies its potent *in vivo* activity in both arthritis and cancer animal models.

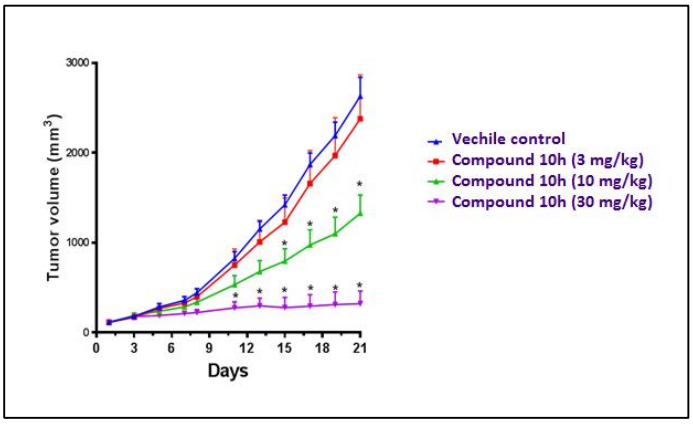


**Figure 23:** *In vivo* anti-tumor activity of Compound **10h**

### 2.3.5. Safety pharmacology study of compound 10h

Daily oral administration of compounds **10h**, at 10X of lowest efficacy dose (10 mg/kg) (as per CIA mice model), over a period of 2 weeks did not affect the survival of Wistar rats, with no adverse effect related to gross pathology, clinical signs, body weight, and food consumption were noticed as compared to the control group. Compound **10h** treated groups showed no changes in the other key organs (brain, heart, kidney, spleen and liver) weights, **Table 10**.

**Table 10:** Relative organ weights (%) after 14 days repeat dose treatment with compound **10h**

| Organs | Compounds | |
|---|---|---|
| | Control (Vehicle) | 10h[a] (100 mg kg$^{-1}$, po, bid) |
| Brain | 0.680±0.025 | 0.665±0.02 |
| Kidney | 0.790±0.034 | 0.805±0.02 |
| Heart | 0.340±0.008 | 0.350±0.007 |
| Spleen | 0.260±0.006 | 0.255±0.01 |
| Liver | 3.580±0.15 | 3.610±0.078 |

[a] Values expressed as mean ± SD: n=9, Male WR, dose 100 mg kg-1, po (bid), 14 days repeated dose toxicity study.

To assure hematological parameter and serum biochemistry, rats were anesthetized 24h post treatment with compound **10h** and blood samples were collected. The whole blood was centrifuged at 3000 rpm, using a centrifuge at 37 $^{o}$C for 15 mins and serum alanine transaminase (ALT), aspartate aminotransferase (AST) and alkaline phosphatase (ALP) were assayed, using a diagnostic kit (Boehringer Mannheim). Total bilirubin (TBILI) was also analysed to check hepatotoxicity parameters.

**Table 11:** Hematological parameters and serum chemistry of compound **10h**

| Parameters | Compound | |
|---|---|---|
| | Control | 10h[a] |
| RBC ($10^6$ $\mu l^{-1}$) | 7.15 ± 0.10 | 7.35 ± 0.28 |
| WBC ($10^3$ $\mu l^{-1}$) | 9.21 ± 0.35 | 9.01 ± 0.28 |
| TBILI (mg $dL^{-1}$) | 0.14 ± 0.10 | 0.15 ± 0.15 |
| ALT (U $L^{-1}$) | 20.10 ± 0.80 | 21.05 ± 1.25 |
| ALP (U $L^{-1}$) | 134.10 ± 6.10 | 122.10 ± 10.40 |
| AST (U $L^{-1}$) | 145.10 ± 10.60 | 138 ± 1.20 |

[a] Values expressed as mean ± SD: n=9, Male WR dose 100 mg kg-1, po (bid), 14 days repeated dose toxicity study

As shown in above table, **Table 11**, the hematological parameters white blood cell (WBC) and red blood cell (RBC) of compounds **10h** were found to be comparable to that of control animals. Similarly, compound **10h** showed no significant changes in ALP, AST, ALT and TBILI as compared to the control group. Whereas Idelalisib has unscheduled death, hepatotoxicity, increased ALT, AST and ALP **[80]**.

### 2.3.6. Molecular modelling study

Further to rationalised the potent and selective PI3Kδ inhibitory activity of **10h**, docking studies were carried out using Glide 5.6 for compounds **9c**,**10h**, **10k** and Dactolisib, **Figure 19**. The PI3Kδ crystal structure was retrieved from the RCSB Protein Data Bank (PDB: **4XE0**). The active site was defined to include residues within 10 $A^{O}$ and the key amino acid residues in binding and specificity pockets are highlighted, **Figure 19**.

As shown in the **Figure 24**, all the three compounds showed favourable interactions with the PI3Kδ ATP-binding pockets, imidazo-quinoline ring served as the hinge binder and it forms key hydrogen bonds with $Val_{828}$ and $Glu_{826}$. However, the Dactolisib makes no interaction with $Trp_{760}$, key residue in specificity pocket. Compound **10h** adopts propeller-shaped conformation where the *p*-methoxy-benzyl-imidazo moiety was found to be sandwiched into the induced hydrophobic specificity pocket between $Trp_{760}$ and $Met_{752}$ and methoxy-benzyl group forms π-π stacking interactions with $Trp_{760}$ in PI3Kδ selectivity pocket, thereby, force the inhibitor to adopt an extended conformation. Also, propeller-shaped conformation of **10h** favours to accommodate methanesulfonamide pyridyl ring of **10h**, in the affinity pocket which strongly interacts with $Asp_{911}$. It appears that an additional hydrogen bonding of **10h** with $Trp_{760}$ and propeller shape orientation contributes towards improved PI3Kδ selectivity and inhibitory activity in this case, While compound **10k** showed weak interaction with $Trp_{760}$ in specificity pocket, affinity region and strong interaction with $Val_{828}$ (hinge region) thereby exhibits good PI3Kδ inhibition but less selectivity as compared to compound **10h**. Compound **9c** showed similar interaction in hinge region with $Val_{828}$,

specificity pocket and hydrophobic region. But interaction in $Asp_{911}$ is weak as compared to compound **10h** due to absence of methanesulfonamide group.

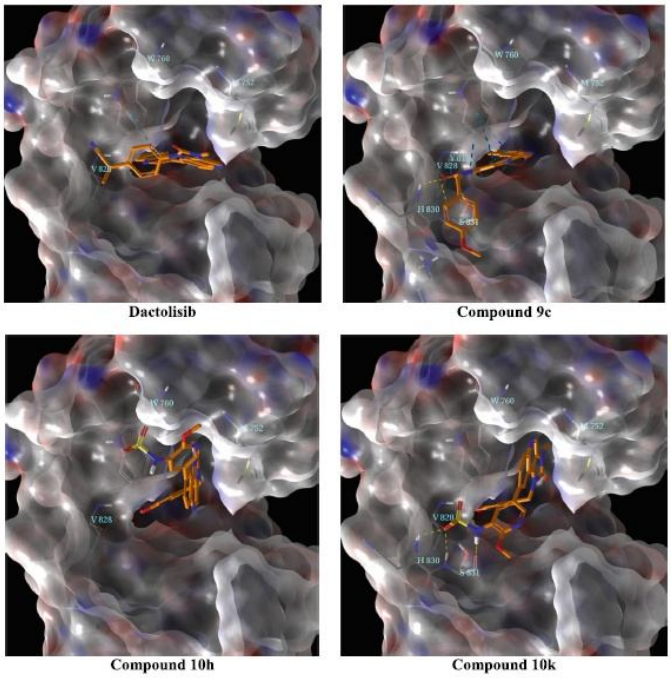


**Figure 24:** The Glide docking studies of Compounds **9c**, **10h**, **10k** and Dactolisib into site of PI3Kδ (PDB ID:4XE0). Compounds are shown as sticks. Hydrogen bonds are shown as yellow dash lines.

## 2.4. Conclusion

In conclusion, we have synthesized and evaluated two sets of novel series of 1,3-dihydro-2*H*-imidazo[4,5-*c*]quinolin-2-one derivatives as selective PI3Kδ inhibitors. In first set, appropriate modifications were carried out in the imidazo-quinoline based pharmacophore, which led to an identification of a single digit nM potent PI3Kδ inhibitor (**9c**), with moderate isoform selectivity.

In set 2, further structure-activity relationship (SAR) studies on the 8$^{th}$ position of **9c** resulted in to the discovery of *N*-(2-methoxy-5-(3-(4-

methoxybenzyl)-1-methyl-2-oxo-2,3-dihydro-1H-imidazo[4,5-*c*]quinolin-8-yl)pyridin-3-yl)methanesulfonamide (**10h**) that showed improved isoform selectivity, PK profile and good efficacy in a CIA and xenograft animal models.

In the repeat dose acute toxicity study, compound **10h** showed no adverse changes related to gross pathology, clinical signs and liver toxicity, Whereas Idelalisib has unscheduled death, hepatotoxicity, increased ALT, AST and ALP. The molecular docking study of compound **10h** indicated key hydrogen bonding interactions, which justifies its selective PI3Kδ inhibitory activity.

Overall pre-clinical data suggest that the development of a potent and selective PI3Kδ inhibitor could be viable therapeutic option for the safe and effective treatment of rheumatoid arthritis and B-cell chronic lymphocytic leukemia.